FRAMBOIDAL PYRITE SHROUD CONFIRMS THE 'DEATH MASK' MODEL FOR MOLDIC PRESERVATION OF EDIACARAN SOFT-BODIED ORGANISMS

ALEXANDER G. LIU

School of Earth Sciences, University of Bristol, Life Sciences Building, 24 Tyndall Avenue, Bristol, BS8 1TQ, U.K. Email: alex.liu@bristol.ac.uk

Keywords: Taphonomy, Newfoundland, Oxygen, Neoproterozoic, Bacterial Sulfate Reduction.

ABSTRACT

The mechanisms by which soft-bodied organisms were preserved in late Ediacaran deep-marine environments are revealed by petrographic and geochemical investigation of fossil-bearing surfaces from the Conception and St. John's groups (Newfoundland, Canada). Framboidal pyrite veneers are documented on fossil-bearing horizons at multiple localities. The pyrite is interpreted to have formed via microbial processes in the hours to weeks following burial of benthic communities. This finding extends the 'death mask' model for Ediacaran soft-tissue preservation (cf. Gehling, 1999) to deep-marine settings. Remineralization and oxidation of pyrite to iron oxides and oxyhydroxides is recognized to result from recent oxidation by meteoric fluids in the shallow subsurface. Consideration of other global Ediacaran macrofossil occurrences

reveals that pyrite has now been found in association with Ediacaran macrofossils preserved in all four previously described styles of moldic preservation (Flinders-, Conception-, Fermeuse- and Nama-type). This suggests that replication of external morphology by framboidal pyrite was a widespread mechanism by which soft-bodied organisms and associated organic surfaces were preserved in multiple facies and depositional environments 580–541 million years ago. The extensive global burial of pyrite in medium- to coarse-grained clastics and carbonates is a previously unrecognized yet potentially significant sink of iron and sulfur, and may have contributed to rising atmospheric and ocean oxygen concentrations across the late Ediacaran interval.

AN INTRODUCTION TO EDIACARAN TAPHONOMY

Late Ediacaran (~580–541 Ma) sedimentary successions host some of the oldest fossils of macroscopic soft-bodied organisms (Narbonne et al., 2012). Such macrofossils can occur in abundances of hundreds to thousands of individuals per square meter (Clapham et al., 2003; Zakrevskaya, 2014; Droser and Gehling, 2015), and are known from over 40 localities worldwide (Fedonkin et al., 2007). The biological affinities and paleoecology of this Ediacaran macrobiota are areas of intense study, but it is widely recognized that many observed morphological and paleoecological signatures may result from taphonomic processes (e.g., Clapham et al., 2003; Droser et al., 2006; Darroch et al., 2013; Liu et al., 2015). Obtaining a comprehensive understanding of the taphonomic history of Ediacaran macrofossils is therefore essential if we are to correctly identify morphological and evolutionary patterns and processes in latest Neoproterozoic marine ecosystems.

The taphonomic history of an organism is influenced by multiple biological, physical, chemical, ecological and sedimentological factors (Fedonkin, 1985), all of which must be considered when interpreting fossil material. In the Phanerozoic, preservation of non-mineralized organisms is largely confined to konservat Lagerstätten of limited spatial extent (e.g., Seilacher et al., 1985; Allison and Briggs, 1993), and typically requires exceptional ambient chemical, physical, or environmental conditions to facilitate soft-tissue preservation (e.g., low oxygen concentrations to exclude metazoan activity, suppress aerobic microbial decay, and provide favourable chemical conditions for soft tissue mineralization and/or casting within the sediment, cf. the Burgess Shale; Allison and Bottjer, 2011; Gaines et al., 2012a; Wilson and Butterfield, 2014).

In contrast, the late Ediacaran Period appears to have been a remarkable interval for the preservation of non-mineralized organisms, which are found globally in a wide range of facies (Seilacher et al., 1985; Butterfield, 2003; Schiffbauer and Laflamme, 2012; Kenchington and Wilby, 2015). Ediacaran macrofossils of soft-bodied organisms have now been described from shelf carbonates (e.g., Siberia and South China; Grazhdankin et al., 2008; Jiang et al., 2011; Chen et al., 2014) and black shales (Grazhdankin et al., 2008; Zhu et al., 2008; Yuan et al., 2011; Wang et al., 2014), in addition to occurrences in siliciclastic successions representing deep-marine basins and slopes (e.g., England, Newfoundland and NW Canada; Narbonne, 2005; Wilby et al., 2011; Narbonne et al., 2014), storm-influenced shoreface environments (Australia and Namibia; Gehling, 1999; Droser et al., 2006; Vickers-Rich et al., 2013), and marginal marine channels and prodeltas (the White Sea of Russia; Grazhdankin, 2004). Intertidal and fluvial settings of this age are generally devoid of macrofossils, with sedimentary structures indicative of microbial activity (e.g., MISS, ‘Arumberia’, or pit-and-mound structures) being the primary biogenic impressions in such facies (Grazhdankin, 2004; McIlroy et al., 2005; Droser et al., 2006; Menon et al., 2016).

Fossil preservation at Ediacaran macrofossil localities has been suggested to fall within three dominant styles: moldic preservation, carbonaceous compressions, and replication by diagenetic minerals (Kenchington and Wilby, 2015). This manuscript focuses on moldic preservation, the taphonomic style responsible for the preservation of macrofossils at classic Ediacaran localities in South Australia, the White Sea, the U.K. and eastern Newfoundland, where it has been known to replicate morphological features <100 μm in dimension (e.g., Narbonne, 2004; Liu et al., 2016). Although moldic impressions can be hosted in carbonates (Grazhdankin et al., 2008; Chen et al., 2014), most Ediacaran examples occur in siliciclastic settings, where four different styles of moldic soft-tissue preservation are recognized by Narbonne (2005). These styles are essentially defined by differences in the casting medium, dependant on whether fossils are preserved on the soles of turbidites (Fermeuse-style preservation), beneath volcanic tuffs (Conception-type preservation), in association with cyanobacterial mats (Flinders-style preservation), or interstratally within siliciclastic sediments (Nama-type preservation; see also Narbonne et al., 2014).

When found on bedding surfaces, organisms can be preserved as positive and/or negative hyporeliefs and/or epireliefs (Glaessner and Wade, 1966), with certain taxa and localities often associated with a particular combination of these (e.g., *Fractofusus* in Newfoundland is typically a negative epirelief impression, whereas *Dickinsonia* in Australia is usually preserved in negative hyporelief; Gehling, 1999; Gehling and Narbonne, 2007). In addition to simple external molds and casts, rare internal molds (Narbonne, 2004), composite molds, and three-dimensional preservation of specimens within beds are also reported (Droser et al., 2006). These taphonomic variants have been ascribed to factors including variability in decay resistance of biological tissues in individual organisms, differential rates of decay relative to rates of sediment compaction, and the presence and type of microbial mats on the original seafloor (e.g., Wade, 1968; Gehling, 1999; Narbonne, 2005). However,

99 the primary controls on late Ediacaran preservation of soft-bodied organisms have remained
100 elusive.

101 Explanations for the profligacy and high-quality preservation of late Ediacaran
102 macrofossils focus on evidence for widespread benthic microbial mats, and a perceived
103 absence of scavengers, predators, and pervasive bioturbating organisms (Fedonkin, 1985;
104 Allison and Briggs, 1993; Callow and Brasier, 2009; Liu et al., 2011). The favoured
105 explanation for late Ediacaran moldic preservation in siliciclastic sediments involves the
106 smothering of paleocommunities on microbe-covered seafloors by event beds (e.g., volcanic
107 ash, or storm sands; Narbonne, 2005), followed by microbially-induced precipitation of pyrite
108 around the organisms (Gehling, 1999; though see Serezhnikova, 2011 for an alternative
109 view). Bacterial sulfate reduction (BSR) is considered to have broken down organic matter in
110 and on buried microbial mats and macro-organisms, producing bisulfide (HS^-) and hydrogen
111 sulfide (H_2S). These compounds then reacted with iron in the sediment (either already present
112 in the pore waters, or generated by microbial Fe-reduction; Berner, 1969; Goldhaber and
113 Kaplan, 1974) to form iron monosulfides on the surface of organic matter, creating a
114 mineralized 'death mask' of its exterior (Berner, 1984; Gehling, 1999; see also Gehling et al.,
115 2005; Droser et al., 2006). Later reaction of these monosulfides with further sulfur led to
116 pyrite formation (Berner, 1984; Gehling, 1999). For pyrite to form within sediments around
117 organic matter, the activity of sulfate reducing bacteria and sources of iron and sulfate are
118 required (Briggs et al., 1996). Even if there is sufficient iron present in the sediment for
119 pyritization to proceed (cf., Farrell et al., 2009, 2013), the activity of iron reducing micro-
120 organisms is often also important to transform that iron from solid Fe(III) to an aqueous
121 Fe(II) phase. Importantly, for pyrite formation to be concentrated around organisms and not
122 diffused throughout the sediment, organic carbon concentrations in the surrounding
123 sediments need to be low, thus restricting microbial reactions solely to the vicinity of the

organisms (e.g., Canfield and Raiswell, 1991; Briggs et al., 1991). Binding and sealing of the sediment-water interface above buried organisms by further microbial mat development would have prevented oxidation of the newly formed sulfides by oxygen-bearing pore fluids (Gehling et al., 2005), enabling preservation of a mineralized moldic replica of the biological tissues. The amount of time a carcass spent within particular microbial zones (dependent on the depth of burial and thus sedimentation rate), may have influenced both the extent of pyritization and the degree of later mineralization or stabilization by other means (e.g., kerogenization; Schiffbauer et al., 2014).

The 'death mask' model outlined above was developed to explain mold and cast preservation in coarse-grained quartzites in South Australia (e.g., Flinders-type preservation of Narbonne, 2005). Sands rarely possess pyritized fossils, since their relatively high porosity and permeability favour oxic respiration, permitting organic carbon to be removed from the system before anoxic conditions (required for pyrite formation) can develop. The 'death mask' model circumvents this issue by proposing that conditions in the sediment shortly after burial were essentially 'closed', due to rapid growth of microbial communities on the seafloor above the buried surfaces forming a barrier to pore water flow from the water column (Gehling, 1999). Despite the apparent success of the model in explaining Ediacaran taphonomic processes, a deep-weathering profile in South Australia prevents examination of primary mineralogy (Gehling et al., 2005), such that primary pyrite sole veneers have yet to be documented from that region. However, support for the 'death mask' model has been offered by mineralogical evidence for an oxidation pathway from pyrite to iron oxides in Australian strata (Mapstone and McIlroy, 2006); red iron oxide staining of many fossil-bearing surfaces (e.g., Wade, 1968); and the casting of negative hyporelief fossil impressions by sediment from layers beneath (Droser et al., 2006). The high quality replication of external morphology in Ediacaran impressions would imply that pyritic 'death masks', or at least their

monosulfide precursors, formed over very short intervals of time (on the order of days to weeks) prior to the decay of the organisms; timescales that we should be able to replicate experimentally. Early experimental attempts to replicate Ediacaran preservational processes largely focused on coarse-grained siliciclastic settings and sediments (Norris, 1989; Bruton, 1991). However, those studies assessed only a limited number of phyla, tissue types, and substrates, and left many important variables unconstrained (most notably by not including microbial mats in the experimental protocol; Kenchington and Wilby, 2015). More recent attempts to re-create a pyritic 'death mask' observed high localized concentrations of Fe and S, assumed to reflect the presence of iron sulfides, and elevated concentrations of aluminosilicate elements, in a black precipitate formed in the vicinity of organic matter undergoing decay on freshwater cyanobacterial mats (Darroch et al., 2012). Those findings are broadly consistent with the early stages of the 'death mask' model, and recognise the importance of sedimentary organic matter in facilitating rapid decay, but failed to generate pyritic 'death masks' of external morphology over short timescales. Pyrite framboids have been recognized in natural systems to form in association with microbial activity (e.g., Popa et al., 2004; MacLean et al., 2008), and have been produced in the laboratory both in *in vitro* cultures enriched with sulfur reducing bacteria (SRB) (Donald and Southam, 1999), and abiotically (e.g., Butler and Rickard, 2000). In the few experimental studies to have produced actual pyrite framboids around buried organic matter (which involved pyritization of plant material), framboids formed over timescales on the order of a few weeks (Grimes et al., 2001; Brock et al., 2006).

In Avalonian deep-marine localities (eastern Newfoundland and the southern UK; Cocks et al., 1997) there have been only rare incidental reports of pyrite on fossil and trace fossil surfaces (Gehling et al., 2005; Liu et al., 2010; Laflamme et al., 2011; Liu et al., 2014a). Consequently, the 'death mask' model has not been widely discussed with respect to

the Fermeuse-type and Conception-type preservation (cf., Narbonne, 2005) typical of the region. Much of the previously observed pyrite is clearly late stage authigenic mineralization, with pyrite cubes several centimetres in dimension found in certain sections (e.g., O'Brien and King, 2005). Microbial surface fabrics have been noted in Newfoundland and the U.K. (e.g., Droser et al., 2006; Brasier et al., 2010), but in the absence of documented mineralized veneers, alternative processes invoking rapid cementation of volcanic ash, or authigenic silicate precipitation, have been considered integral to the Avalonian preservation process (Narbonne, 2005; Callow and Brasier, 2009).

Here, a detailed petrological study recognises widespread pyrite-associated mineral veneers on fossil-bearing bedding planes from Newfoundland, confirming the applicability of the 'death mask' model (Gehling, 1999) to Ediacaran macrofossil preservation in Avalonian marine siliciclastic settings. This finding implies that moldic preservation of late Ediacaran soft-bodied organisms may have been governed by a common global mechanism; a suggestion that has implications for our understanding of late Ediacaran taphonomic processes, and the nature of early burial environments.

MATERIALS AND METHODS

Sedimentary samples were collected from fossil-bearing bedding planes on the Avalon and Bonavista peninsulas, Newfoundland, Canada (Fig. 1). All studied sites are protected by provincial legislation, and lie under the jurisdiction of either the Parks and Natural Areas Division of the Department of Environment and Conservation (for Mistaken Point Ecological Reserve; MPER), or the Department of Business, Tourism, Culture and Rural Development (elsewhere in the Province, as outlined in Regulation 67/11 of the Historic Resources Act,

197 2011). Collection of sedimentary samples may only be undertaken under permits issued by
198 the bodies above, while collection of Ediacaran fossil material is strictly prohibited.

199 Sedimentary samples were chosen to include both the green-weathering siltstone
200 (interpreted as hemipelagites; cf., Liu et al., 2014b) upon which fossil assemblages are
201 impressed, and the ash or smothering sediment that covered them. Standard polished,
202 uncovered thin sections were made through sedimentary samples perpendicular to the
203 bedding surfaces. Since the smothering sediments in the collected samples have not
204 weathered off to reveal their underlying surfaces, it is not possible to know whether
205 macrofossils lie in the investigated planes of section. For the purposes of this manuscript, it is
206 assumed that they do not, and all observations are considered to be indicative of conditions
207 across the entire bedding surface. A selection of thin sections were carbon-coated and
208 underwent imaging, energy dispersive spectrometer (EDS) mineral characterization, and
209 quantitative elemental mapping on a Hitachi S-3500N variable pressure Scanning Electron
210 Microscope (SEM) equipped with Thermo Noran EDS x-ray detector, and Cameca SX-100
211 electron microprobe, at the School of Earth Sciences, University of Bristol. All raw files
212 relating to the elemental maps, SEM images, and EDS point analyses are stored in the Bristol
213 Data Repository: http://data-bris.acrc.bris.ac.uk/deposits/1rdlayqk8sje91lk0iq1mdnzib
214 Thin sections from nine localities are presented here to demonstrate the variation
215 inherent within the study area (Fig. 1). The nine sites are the Brasier (aka BR5) Surface, the
216 Pigeon Cove 'pizza disc' surface, and the 'E' Surface from Mistaken Point Ecological
217 Reserve; the '3D' rangeomorph surface at Spaniard's Bay (SB); and the H14, LC6, LC13,
218 MEL7 and MUN surfaces on the Bonavista Peninsula (Fig. 1; names of surfaces follow field
219 notebook terminology). Taken together, these surfaces span the Drook to Fermeuse
220 Formations of the Conception and St. John's groups (following the lithostratigraphic
221 correlation of Ichaso et al., 2007, and Hofmann et al., 2008), and exhibit a broad range of

preservational quality. The BR5 and 'E' Surfaces were sampled at multiple locations along each bedding plane, at distances of up to 20 m (on 'E') and 100 m (BR5) apart, to determine the lateral continuity of sedimentary characteristics across individual surfaces. Further sedimentological and stratigraphic information regarding these surfaces can be found in the Supplementary Information file. All studied thin sections reside at the Department of Earth Sciences, University of Cambridge.

Geological Context

Eastern Newfoundland hosts some of the world's oldest Ediacara-type macrofossils (Narbonne and Gehling, 2003), with hundreds of fossil-bearing surfaces spanning a ~20 million year interval ~579–560 Ma (dating after Benus, 1988; Van Kranendonk et al., 2008). Fossils are preserved beneath volcanic tuffs, volcaniclastic sediments, or sandy turbidites, largely as positive or negative epirelief impressions of the exterior surfaces of the organisms (cf., Liu et al., 2011 and references therein). Strata of the Conception and St. John's groups are predominantly turbiditic, deposited in marine basin and slope environments offshore from an active volcanic arc (Wood et al., 2003). Importantly, there is no evidence of shallow water (above wave base) deposition throughout the entire fossil-bearing succession from the Drook to lower Fermeuse Formations (Wood et al., 2003); where shallow-water indicators do appear in the upper Fermeuse Fm. and the Signal Hill Group, non-discoidal macrofossils are not observed. The entire volcaniclastic succession has been interpreted as a flysch-molasse transition (Myrow, 1995). Fossils occur within turbidite successions on thin, green-weathering, siltstone beds interpreted as contourites or hemipelagites (Supp. Fig. 2A; Wood et al., 2003). Detailed accounts of the sedimentology and facies associations in the Ediacaran strata of the Avalon and Bonavista peninsulas have been published in recent years (Wood et

al., 2003; Ichaso et al., 2007; Mason et al., 2013). Folding and faulting is pervasive within the Avalon region, and some units have undergone prehnite-pumpellyite low-grade metamorphism (Papezik, 1974). The paleobiological and paleoecological attributes of the fossil assemblages have been recently reviewed by Liu et al. (2015).

RESULTS

For ease of interpretation, it is useful to define descriptive terms to permit direct comparison of sedimentary samples from different sites:

Under-bed: the sedimentary substrate upon which the organisms were living. In the Conception Group of Newfoundland, this is usually a green-weathering hemipelagite (Supp. Fig. 2A), the top surface of which is often stained red (Supp. Fig. 1) and bears positive and negative epirelief fossil impressions (e.g., Supp. Fig. 2B).

Over-bed: the event bed that smothered a given Ediacaran community. Typically this is a volcanic tuff, a volcaniclastic sediment, or more rarely, the base of a sandy or silty turbidite.

Veneer: a thin (typically <1 mm thick), laterally continuous layer present at the interface between the under-bed and over-bed, predominantly composed of iron-bearing minerals. The veneer is typically situated within the base of the over-bed.

Petrology and SEM Analysis

Under-bed.—Fossils generally occur on green-weathering siltstone layers of up to 7 cm in thickness. These siltstone layers lie above the T_e unit of the underlying turbidite, with which they possess a sharp contact (Supp. Fig. 2A). Under-bed siltstones are relatively consistent in

mineralogy and sedimentology in all studied sections (Fig. 2), being siliciclastic with grain size typically <30 μm, and composed of feldspars, quartz, clay minerals and phyllosilicates. The siltstones often bear a mottled appearance due to the presence of millimetric lenses of coarser quartz-rich silt (Landing et al., 1988), although the abundance of these clusters within the under-bed can be quite variable between localities (Fig. 2). Such siltstones are inferred to represent either sedimentation of pelagic material accumulated in the intervals between turbidity current flows, or contourite deposits (the latter interpretation informed by frequent alignment of many frondose fossils on the surfaces perpendicular to the downslope direction indicated by ripples in underlying turbidites; Narbonne et al., 2005; Narbonne et al., 2014). Baffling of coarser grains by microbial mats, or biological processing of the sediment, may offer alternative explanations for the mottled textures.

Over-bed.—The most obvious difference in petrology between the studied fossil-bearing surfaces is the mineralogy and grain size of the over-bed. This varies considerably from fine silt-sized grains of volcaniclastic material (e.g., on the MUN Surface; Fig. 2A) that have undergone little alteration or metamorphic overprint, to coarse sand-sized clasts of altered volcanic origin within a pervasive chlorite matrix (e.g., the ash fraction directly above the Mistaken Point 'E' Surface; Fig. 2D). Many of the tuffs in the Conception Group possess mineralogies consistent with dacitic and andesitic compositions (Retallack, 2014). However, later alteration has almost certainly affected both the observed mineralogy and grain size of the matrix in several cases (e.g., via dissolution of volcanic glass and increase in the clay mineral component; Kiipli et al., 2007; Page et al., 2008).

Mineralized veneer.—A thin (15 μm to 1.5 mm) veneer of opaque minerals is commonly observed at the interface between the under-bed and over-bed on fossil-bearing surfaces (Fig. 2). Veneers can vary in thickness quite substantially over small distances, and constituent minerals are typically spherical (2–25 μm diameter), and confined to the over-bed side of the interface (Supp. Figs S3A–E, 4–6). Mineralogy of the veneer varies between and even within individual samples, with iron oxides and oxyhydroxides being the dominant phases (as confirmed by SEM EDS; Supp. Figs 7–10). Importantly, some beds (e.g., BR5) have veneers composed of framboidal, microcrystalline pyrite (see also the Elemental Mapping section below; Figs 3–5; Supp. Figs 6–7, 9). Sedimentary grains can be caught up within the veneer, but these comprise <50% of the material within the veneer margins. On bed BR5 (Briscal Formation of Mistaken Point Ecological Reserve), sedimentary samples taken ~100 m apart reveal that the mineralized veneer is broadly consistent in thickness and general appearance across that surface (compare Figs 4A–B with 4C–D, see also Supp. Fig. 5). However, the BR5 veneer has a different mineralogy in the two studied thin sections, being entirely pyritic in one sample (BR5 2013), and composed of iron oxide with minor pyrite regions in the other (BR5 2014) (Figs 4A–D; Supp. Figs 5–7). These observations demonstrate that the veneer is a consistent and continuous feature across the fossil-bearing surfaces, but that its mineralogy can vary.

Bed BR5 reveals that framboid morphology within a veneer can also vary. In region II of sample BR5 2013, closest to the interface with the under-bed, all pyrite is in the form of discrete pyrite framboids, or ‘exploded’ microcrystalline pyrite patches (Fig. 3E). In contrast, in region III of the veneer, which is separated from region II by a ~100 μm thick layer of framboid-poor sediment (Fig. 3C), all pyrite framboids have an outer rim of blocky, coarser crystalline pyrite (Fig. 3D). This rim extends only one crystal width (2–6 μm) around the exterior of the framboid, and can often be seen in SEM images as an empty ‘ring’, where the

original framboid has been plucked out during the polishing process, leaving the blocky pyrite rim behind (Fig. 3D, centre-right).

A thin section from bed LC6 (Trepassey Formation of the Bonavista Peninsula), reveals interesting variation in veneer mineralogy over a very small distance (Fig. 4E). The veneer minerals here can be pyritic in one area of a thin section, but progressively more blocky and oxidised in other regions of the over-bed just a few hundred microns away (Fig. 4E; Supp. Figs 3E, 9). Furthermore, oxidation of individual grains appears to progress from the outside of the framboid towards its centre (Fig. 4E).

In outcrop, veneers can occasionally be recognized as 'rusty' mineralized layers on bedding plane surfaces (e.g., Fig. 3A–B; Liu et al., 2016 supp. fig. 3A). Such rusty layers can also be found quite abundantly at the interfaces between turbidites in certain sections (e.g., the upper Drook Formation, Supp. Fig. 2C–D), demonstrating that volcanic tuffs are not required for their formation. Horizontally aligned and laterally discontinuous 'wisps' of spherical minerals are also occasionally observed within the under-bed, at depths of a few millimeters to several centimeters beneath the main veneer (e.g., Fig. 2F). These wisps are typically only a few tens of microns thick and a few millimeters in length (e.g., the Spaniard's Bay Surface, Fig. 2F), with individual grains possessing identical mineralogies and morphologies to those forming veneers at higher levels within the thin section.

The only major fossil horizons where a clear mineralized veneer was not observed are the Mistaken Point 'D' and 'E' Surfaces. The 'D' and 'E' Surface over-bed tuffs show clear evidence of chloritization and replacement of several mineral phases (e.g., Fig. 2D), which results from low-grade metamorphism and later weathering (Papezik, 1974). Occasional crystals of rutile and haematite are also observed at the base of the 'E' Surface tuff (Fig. 2D). It is possible that the iron now bound within these minerals, and in the abundant chlorite in the over-bed matrix, originated from primary pyrite framboids located along the sedimentary

342 interface. The lack of a mineralized veneer on this horizon is consistent across the exposed
343 bedding plane (confirmed by study of thin sections taken from areas 20 m apart). However, it
344 must be noted that it was not possible to obtain a pristine, unweathered sample from either of
345 these surfaces.
346
347 ## Elemental Mapping
348 Elemental maps were made of small regions of the mineralized veneer in three thin sections
349 (BR5 2013, MUN, and LC6; Fig. 5). These maps permitted distinction between the main
350 mineral phases present in the sections. Spherical grains within the mineralized veneers are
351 confirmed to be either pyrite (bed BR5), iron oxide (MUN), or a combination of the two
352 (LC6), with iron oxide replacing pyrite grains in higher levels of the veneer in the latter
353 section. An iron-rich, subtly layered mineralized crust is observed above the main veneer on
354 bed BR5, and is considered to result from modern weathering and secondary precipitation of
355 abundant iron oxides over the exposed surface (Fig. 5).
356
357 # DISCUSSION
358 Thin sections through fossil-bearing horizons in Newfoundland reveal a close association
359 between mineral veneers and fossil-bearing surfaces throughout the late Ediacaran marine
360 succession. The majority of studied fossil-bearing surfaces possess a mineralized veneer
361 immediately above them (Fig. 2). Where present, the veneer is variously composed of
362 framboidal pyrite, spherical clusters of blocky pyrite, or a mixture of spherical iron oxides
363 and hydroxides of similar shape and dimension to pyrite framboids (Figs 4–5). On beds
364 where multiple samples were taken from different locations on the same surface,
365 mineralogical characteristics and relative thickness of sedimentary layers and veneers were
366 consistent, apart from on bed BR5 where spherical mineral aggregates were pyritic in one

thin section, but oxidised in the other (Fig. 4A–D; Supp. Figs 5–7). Further evidence from bed BR5 demonstrates that framboidal pyrite within veneers has in places undergone secondary 'coating' by overgrowths of blocky pyrite (Fig. 3D, consistent with recent and ancient observations of pyrite overgrowth; Wacey et al., 2015). Meanwhile, bed LC6 documents oxidation of pyrite framboids to iron oxides within an individual thin section (Fig. 4E), with oxidation proceeding from upper to lower levels within the veneer, and from rim to core in individual framboids. Together, these observations suggest that the observed oxidation is occurring due to modern weathering processes involving meteoritic water.

The similarities in diameter, morphology, and fabric of the spherical mineral aggregates comprising the veneers in non-pyrite-bearing thin sections suggest they are likely to have originally been pyrite framboids. It is therefore proposed that the entire surfaces on which Ediacaran fossils are preserved in Newfoundland were coated with a thin pyritic veneer soon after burial. In some cases, this veneer has subsequently oxidized to iron oxides and other iron species, consistent with widespread red-staining of fossil surfaces at many sites in both Newfoundland and Australia (Supp. Fig. 1; Droser et al., 2006), and with the 'death mask' model (Gehling, 1999). The veneers represent the first direct evidence for the presence of laterally continuous pyritic veneers on Ediacaran fossil-bearing surfaces.

Formation of the veneers.

Many authors have attempted to explain the formation of framboidal pyrite, and multiple biological and abiological pathways are now recognized (Schallreuter, 1984; Wilkin and Barnes, 1997; Butler and Rickard, 2000; Rickard, 2012; Wacey et al., 2015). Key steps in the bacterially-mediated biological production pathway are: (1) breakdown of organic matter to smaller particles in the presence of dissolved sulfate, which is reduced to H_2S; (2) reaction of

391 H_2S with reactive iron ions in pore fluids to produce iron monosulfides; and (3) reaction of
392 these monosulfides (e.g., FeS) with sulfur ions to form pyrite (Berner, 1970, 1984).

393 Formation of framboidal pyrite in enriched cultures of SRB reveals that biogenically-
394 produced FeS precipitates as a nano-scale film on the external surfaces of individual bacteria.
395 Additional H_2S released by cell autolysis is then immobilized at the cell surface and reacts to
396 form microcrystalline pyrite (Donald and Southam, 1999). Subsequent pyrite growth extends
397 out from the cell exterior. The microbial breakdown of organic matter from both the surfaces
398 of Ediacaran macro-organisms, and from contemporaneous benthic microbial mats (the only
399 way the lateral extent of the observed veneers can be explained), is predicted to have begun
400 in similar fashion before extending out into the adjacent sediment (cf., Steiner and Reitner,
401 2001; Wang et al., 2014).

402 Fossil evidence for microbial consortia within the Conception Group of
403 Newfoundland includes surficial microbial mats (e.g., Brasier et al., 2010 fig. 6a), and rare
404 microfossil remains of bacterial organisms (Hofmann et al., 1979). Recently acquired sulfur
405 isotope data present independent evidence for the activity of sulfate reducing micro-
406 organisms associated with the observed mineralized veneers. Un-oxidised pyrite framboids
407 from the MEL 7 fossil surface veneer (Fig. 2E) yield $\delta^{34}S$ values ranging from -15.2‰ to -
408 24.3‰ (mean = -21.5‰; n = 33; data presented in Wacey et al., 2015), indicating
409 fractionation of sulfur isotopes ($\Delta^{34}S$) of up to -50‰ with respect to estimated
410 contemporaneous seawater sulfate isotopic compositions (+25‰; Fike et al., 2006). The
411 magnitude of these fractionations suggests the sulfur in veneer framboids underwent
412 biological processing by microbial sulfate reduction (perhaps in conjunction with limited
413 electron donor supply; cf., Leavitt et al., 2013), prior to incorporation within pyrite framboids
414 (Wacey et al., 2015). Distinct CN_{org} enrichments around framboid microcrystals within the

MEL7 mineral veneer, indicative of formation within a biofilm (Wacey et al., 2015), further support the suggestion that veneer pyrite results from microbial sulfate reduction.

In order for the external morphology of Ediacaran macro-organisms to be coated and cast by framboidal pyrite, the tissues must have remained intact for long enough that SRB could produce sufficient pyrite, or at least precursor iron sulfides (e.g., Sweeney and Kaplan, 1973), to cast them. However, mineralization must have been completed before decay proceeded far enough to efface morphological detail (Briggs, 2003). The timescale over which BSR and mineralization occurred is thus dependent on the rate at which H_2S is produced by microbial activity; the quantity of available organic carbon; the rate of bacterial decay; and the flux of sulfate and dissolved iron to the site of microbial activity (Jørgensen, 1977; Boudreau and Westrich, 1984; Westrich and Berner, 1984). All of these factors are in turn dependent on the depth of the redox zone (controlled in part by the degree of microbial sealing; Gehling et al., 2005; Droser et al., 2006; Callow and Brasier, 2009; Menon et al., 2016), and the mineralogy of the surrounding sediments. The absence of bioturbators and scavengers, which would have disturbed and irrigated the sediment, oxidizing any sulfides, appears to have been significant to the 'death mask' process, enabling sulfides to remain stable and undisturbed. The observation that pyrite framboids are largely confined to the over-bed in Newfoundland may result from a combination of the sediment within the under-bed being separated from the decaying carcasses by a microbial biofilm/mat, and the over-bed typically having a higher porosity due to its coarser grain size.

Oxidation of the pyrite framboids within veneers is likely to result from modern processes, as evidenced by examples of pyrite and iron oxides within the same surface veneer, separated on a variety of scales from microns to meters (Fig. 4). Pyrite oxidation is discussed in an extensive literature on acid rock drainage (e.g., INAP, 2014). Although multiple steps are involved in this process (Stumm and Morgan, 1981; Lowson, 1982;

Rimstidt and Vaughan, 2003), the chemical reaction in natural environments can be simplified to:

$$4FeS_2 + 13O_2 + 2H_2O \rightarrow 4FeSO_4 + 2H_2SO_4 + 2SO_2$$

In aqueous systems (such as those typically found on the coastline of Newfoundland where water commonly flows along bedding interfaces), the oxidation of pyrite by ferric iron can also occur:

$$FeS_2 + 14Fe^{3+} + 8H_2O \rightarrow 15Fe^{2+} + 2SO_4^{2-} + 16H^+$$

The production of sulfuric acid via these processes may be relevant to studies of observed variation in preservational quality of Ediacaran fossils on many surfaces, and is an area of active research. In addition to common iron-bearing oxides, more exotic oxidation products can also be observed. Laser Raman analysis identified the iron sulfate mineral bukovskyite ($Fe_2(AsO_4)(SO_4)OH.7H_20$) forming remineralized rims around pyrite wisps at the Spaniard's Bay fossil locality (Brasier et al., 2013, fig. S3). Bukovskyite is a common alteration product of arsenopyrite (FeAsS), which may have formed as a result of enhanced heavy metal dissolution related to acid rock drainage (Saria et al., 2006).

The global ubiquity of the pyritic 'death mask'

Volcanic ash has often been cited as the primary agent of preservation in Newfoundland (Narbonne, 2005), but the observed variation in over-bed substrate demonstrated in this study (Fig. 2) suggests that this is not the case. Previous suggestions that pyrite might have played a role in macrofossil preservation in Newfoundland are limited to elevated Fe and S concentrations in sediments surrounding *Aspidella* fossils in the Fermeuse Formation (Laflamme et al., 2011), and rare pyrite in bedding-parallel wisps and euhedral blocky

463 crystals associated with macrofossil-bearing horizons at Spaniard's Bay (Brasier et al., 2013
464 fig. 3C–F) and Back Cove (Liu et al., 2014a; Wacey et al., 2015). The results presented
465 herein demonstrate that microbially-formed pyrite veneers are ubiquitous immediately above
466 fossil-bearing surfaces in Newfoundland, revealing that Gehling's 'death mask' model is
467 applicable to deep-marine settings. The findings also raise the possibility that unfigured
468 structures historically assigned to the microfossil taxon *Bavlinella* from the St. John's Group
469 (Timofeyev et al., 1980; Anderson et al., 1982) may actually record pyrite framboids.

470 Consideration of other global Ediacaran macrofossil localities reveals abundant
471 evidence for the involvement of pyrite in fossil preservation in a variety of facies. Pristine
472 pyritized microfossils, bed soles, and mat fabrics have been reported from the White Sea of
473 Russia (Steiner and Reitner, 2001; Dzik, 2003; Grazhdankin, 2003; Grazhdankin and Gerdes,
474 2007), and potentially from Ukraine (Dzik and Martyshyn, 2015). Pyrite framboids are
475 present on the surfaces of carbonaceous compression macrofossils of the Miaohe and Lantian
476 biotas of China (Wang et al., 2014); on pyritized members of the Gaojiashan biota (Cai and
477 Hua, 2007; Cai et al., 2012); and preserving three-dimensional fronds (Steiner and Reitner,
478 2001; Ivantsov, 2016) and other taxa preserved as impressions (Fedonkin and Waggoner,
479 1997; Serezhnikova, 2011) in siliciclastic sediments from the White Sea. Framboidal pyrite is
480 also associated with Ediacaran Sabelliditids from the East European Platform
481 (Moczydłowska et al., 2014). Meanwhile, acritarchs and filamentous microfossils from
482 siliciclastic settings in the Australian Centralian Superbasin (Grey and Willman, 2009), and
483 from siltstones, dolostones and mudstones of the Chinese Yangtze Gorges (Anderson et al.,
484 2011), are preserved in close association with framboidal pyrite. The latter region
485 additionally sees the growth of centripetal pyrite around microbial mat fragments, forming
486 pyrite rims around the silica cortices of chert nodules in Doushantuo Formation shales (Xiao
487 et al., 2010).

Iron oxide veneers considered to result from the secondary oxidation of pyrite are frequently seen coating bedding planes, bed soles, and fossils in the Australian Flinders Ranges (Gehling, 1999) and Amadeus Basin (haematite and clay veneers; Mapstone and McIlroy, 2006), as well as in Newfoundland (Supp. Fig. 1). A paucity of published data on the petrography of the June Beds in NW Canada (Narbonne et al., 2014) precludes determination of whether pyrite mineralization is also responsible for the interstratal preservation of Ediacaran macrofossils there. Oxidation products of pyrite (e.g., jarosite, limonite and goethite) have been observed alongside rare authigenic pyrite encrusting three-dimensionally preserved macrofossil specimens in Namibia (Hall et al., 2013; Vickers-Rich et al., 2013; Meyer et al., 2014a). It is worth noting that the oxidation of pyrite to jarosite involves a 115% increase in molar volume (Lowson, 1982 and references therein), potentially explaining how Ediacaran fossil impressions preserved within beds can become naturally dissociated from the surrounding bedrock upon exhumation, despite there being only limited lithological contrast between the specimen and substrate.

These numerous examples demonstrate that framboidal pyrite and its oxidation products are found in close association with Ediacaran macrofossils preserved as molds and casts throughout the late Ediacaran Period, occurring across entire microbial surfaces in disparate facies, multiple geographic locations, and in both shallow- and deep-marine environments between 579–541 Ma. Although evidence for pyrite has not yet been documented at every late Ediacaran fossil locality (e.g., Rowland and Rodriguez, 2014), it does seem that early diagenetic pyritization played a significant role in the moldic preservation of Ediacaran soft-bodied macro-organisms. This has important implications for previous views on Ediacaran taphonomy, since fossils preserved in Nama-, Fermeuse-, Flinders-, and Conception-styles (cf., Narbonne, 2005) have all now been recognized in association with pyrite or its modern oxidation products, implying that the distinctions

between these taphonomic modes are largely lithological, and that the first-order biological and chemical processes responsible for Ediacaran macrofossil preservation are globally uniform. The alternative suggestion that different preservation pathways result from the activities of different microbial communities (cf., Narbonne, 2005) does not seem parsimonious, but could in future be tackled via experimental investigation. SRB are likely to have been responsible for sulfide generation in all recognized cases, and while other microbes present on the seafloor may not have engaged in sulfate reduction themselves, their organic matter would have contributed organic carbon for SRB to metabolise. Furthermore, it is clear that association of macrofossils with pyrite is not restricted to fine grained facies as in the Phanerozoic, but is commonly seen in Ediacaran coarse-grained clastics and even carbonates. Furthermore, Ediacaran carbonaceous compressions and environments hosting microfossils also exhibit pyritic material.

In Namibia and Australia, Ediacaran macrofossils preserved as three-dimensional external moulds within sandstones (Wade, 1968; Pflug, 1972) have been interpreted as either endobenthic organisms (cf., Seilacher, 1992; Grazhdankin and Seilacher, 2005), or epibenthic organisms incorporated within the sediment during transport and burial (Jenkins, 1992). Such specimens imply that microbial growth coated the entire organisms within the sediment, and the presence of a surficial microbial mat was thus not essential to the preservation process (cf., Callow and Brasier, 2009). Similarly in Newfoundland, preservation of the upper surfaces of fronds and stems (e.g., *Charniodiscus*; Laflamme et al., 2004), and of rangeomorphs in sediment scours beneath the level of the contemporaneous seafloor and its microbial surfaces(Brasier et al., 2013), also indicate that contact of the organisms with a pre-existing mat was not a pre-requisite for pyrite formation.

In combination with distinct marine chemical conditions (summarised in Narbonne et al., 2012; Sperling et al., 2015), the absence of burrowers, scavengers and predators is

considered to have favoured *in situ* preservation of non-mineralized biological structures, including soft-bodied organisms, in the Ediacaran (e.g., Callow and Brasier, 2009). The globally extensive onset of vertical burrowing in the Cambrian (e.g., Seilacher and Pflüger, 1994; Bottjer et al., 2000; Mángano and Buatois, 2014) has thus been considered to have disrupted benthic microbial communities (Buatois et al., 2014; Carbone and Narbonne, 2014) and oxidised sediments to greater depths, bringing an end to 'closed system' conditions. Several studies have proposed that disturbance of microbial mats by motile organisms could have initiated the closure of the Ediacaran taphonomic window, marginalizing soft-tissue preservation towards sites with atypical ambient conditions (cf., Allison and Briggs, 1993; Orr et al., 2003; Brasier, 2009; Laflamme et al., 2013; though see Tarhan et al., 2015). However, microbially-bound substrates with no evidence for associated Ediacara-type macrofossils are now recognised to persist into the Cambrian in several locations (e.g., Dornbos et al., 2004), including in association with abundant pyrite and microbially induced sedimentary structures in the basal Cambrian strata of the Burin Peninsula of Newfoundland (Buatois et al., 2014). If this pyrite formed from original framboidal precursors via similar pathways to those described from the Conception and St. John's groups, it may imply that the 'death mask' taphonomic window extended beyond the Ediacaran Period. The apparent absence of Ediacara-type macrofossils in Member 2 of the Chapel Island Formation could thus be interpreted as evidence for the original absence of such organisms, at least in the specific Cambrian facies represented by those sections (cf., Buatois et al., 2014, though see also Laflamme et al., 2013, and Darroch et al., 2015). Reports of potential examples of predation and bioturbation in deposits coincident with Ediacara-type fossils ≤553 Ma (Bengtson and Zhao, 1992; Rogov et al., 2012; Chen et al., 2013; Meyer et al., 2014b) also raise questions regarding the confounding influence of these activities on latest Ediacaran taphonomy. When coupled with paleoecological data, these observations suggest that the

disappearance of the Ediacaran macrobiota is not simply an artefact of taphonomy (Darroch et al., 2015).

Since the size of authigenic mineral crystals may limit preservational quality in soft tissue replication (Martill, 1998; Briggs, 2003), the preservation of Ediacaran macrofossils beneath coatings of pyrite framboids may impose a limit on the smallest morphological features that can be preserved: the smallest pyrite crystals observed in association with fossils elsewhere in the geological record are ~0.25μm (Grimes et al., 2002). The 'death mask' style of moldic preservation would also only record internal morphology if BSR took place internally within the organism (for example within specific organs or tissues, or in punctured or collapsed specimens); if the external morphology draped topographic high-points of internal structures (as proposed for example by Dzik, 2003); or if early diagenetic conditions facilitated continued BSR and pyritization for significant periods of time (Raiswell et al., 1993; Schiffbauer et al., 2014). As with Phanerozoic assemblages of similarly preserved pyritized fossils, a lack of evidence for internal tissues in Ediacaran moldic macrofossils cannot be taken to imply that they were not present.

INSIGHTS INTO EDIACARAN MARINE CONDITIONS

Pyritization of soft tissues via formation of framboidal pyrite veneers is not unique to the Ediacaran Period, and insights into the preservation process can be gleaned from Phanerozoic studies. The primary difference is that in the Phanerozoic, pyritization is usually spatially restricted to only the area immediately surrounding organisms, and is typically documented in fine-grained clastic successions, whereas in the Ediacaran, pyritization often extends across entire bedding surfaces, in a range of different lithologies. Early diagenetic, bacterially-mediated framboidal pyrite has been demonstrated to play a role in the

preservation of soft tissues in Cambrian arthropods (e.g., Gabbott et al., 2004; Moore and Lieberman, 2009); in localities such as the Ordovician Beechers Trilobite Bed (Briggs et al., 1991); and the Devonian Hunsrück Slates (Briggs et al., 1996; Bartels et al., 1998). Framboidal pyrite has also been found associated with ammonites from the Lias (Hudson, 1982). In such instances it has been suggested that four factors are critical in facilitating this taphonomic mode: rapid burial, a sizeable source of organic matter but minimal organic material in surrounding sediments, and sufficient concentrations of sulfate and iron (Briggs et al., 1996; Farrell et al., 2009; Schiffbauer et al., 2014). The following discussion briefly outlines how these four criteria were achieved over the 40 million year duration of the late Ediacaran moldic taphonomic window.

Rapid burial and anoxia.—Many Ediacaran cast-and-mold-type fossil localities occur in facies that clearly record rapid burial of organisms beneath, or occasionally within, episodic event beds such as storm deposits, turbidites, volcaniclastic events or ash falls (Narbonne, 2005). Oxygen from the water column would not have penetrated the substrate to any great depth following burial due to the thickness of overlying sediment, subsequent sealing of that sediment by microbial growth on the seafloor above (Jørgensen, 1977; Gehling, 1999; Droser et al., 2006), and a general absence of bioturbating organisms (though note Rogov et al., 2012). Consumption of any available oxygen by decomposition would therefore have led to the rapid development of low oxygen conditions beneath the sediment-water interface following burial of organic matter. However, for framboidal pyrite to form, sediments must be in contact with the water column if seawater sulfate is to be exchanged (Raiswell, 1982). It is possible that the rapid burial at Ediacaran sites played a dual role, on the one hand limiting oxygen availability and providing the low oxygen conditions (facilitating sulfide formation via BSR), but on the other, hindering ion exchange and ultimately limiting the time interval

612 over which decay and BSR could operate, constraining the spatial extent of pyritization. The
613 formation of oxygen-poor conditions by rapid burial may also have limited the activity of
614 sulfur oxidizing bacteria, which may otherwise have oxidised sulfides and prevented pyrite
615 formation.

616

617 *Organic matter*.—The distribution of labile organic matter has long been recognized as
618 critical in the pyritization of soft-tissues (e.g., Berner, 1969, 1970; Briggs et al., 1996). In
619 modern sulfate-rich environments, organic matter is typically the rate-limiting factor
620 governing BSR and thus pyrite formation (Berner, 1984). In the geological record,
621 pyritization of macrofossils is favoured in sediments where ambient organic matter is scarce,
622 permitting microbial activity to be focused around carcasses (Briggs et al., 1996; Farrell et
623 al., 2013). Extremely low total organic carbon values reported from bulk sampling through
624 the Conception and St. John's groups in Newfoundland (Canfield et al., 2007) are consistent
625 with this scenario. The organic matter sourced from extensive microbial mats, coupled with
626 the decaying Ediacaran macrobiota (comprising some of the first large, discrete carcasses in
627 the geological record, which may have played a role in driving the evolution of bilaterians;
628 Budd and Jensen, 2015), would therefore have provided a significant organic resource that
629 would have been confined to discrete sedimentary levels within otherwise organic-poor
630 event-beds.

631

632 *Reactive Iron.*—Iron is fundamental to the 'death mask' process, and high dissolved iron
633 concentrations are required to pyritize large carcasses (Raiswell et al., 1993). In modern
634 settings, iron availability is typically the limiting factor on pyrite formation only in euxinic

conditions (Berner, 1984), but it is worth considering reactive iron abundance in the latest Neoproterozoic.

The Ediacaran deep oceans are widely considered to have been ferruginous (and anoxic) throughout much of the Proterozoic (Canfield et al., 2008; Halverson et al., 2009; Lyons et al., 2009; Guilbaud et al., 2015; Sperling et al., 2015), with ferruginous conditions persisting in some deep basins into the late Ediacaran (e.g., Li et al., 2010), albeit with increasingly dynamic variation in redox conditions (Wood et al., 2015). However, the surface and mid-depth environments in which the majority of Ediacaran macrofossils were preserved are considered to have been oxygenated by the late Ediacaran (Canfield et al., 2007; Lyons et al., 2014). Bulk sampling of the Conception Group in Newfoundland yielded high levels of highly-reactive (i.e., unsulfidized) iron (Fe_{HR}) within the sediment (Canfield et al., 2007), implying that the original pore waters of these sediments possessed a plentiful source of iron, which could migrate to react with microbially-produced H_2S at bed interfaces. It is possible that these high iron concentrations in the pore waters could have trapped sulfate at the site of decay (cf., Beecher's Trilobite Bed, Raiswell et al., 1993), facilitating localized soft tissue preservation.

Although a source of iron is easy to envisage in Ediacaran volcaniclastic settings such as Newfoundland with abundant volcanic glass that can be readily dissolved to liberate Fe (cf., Duggen et al., 2010; Gaines et al., 2012b), in sediments with few potential iron-bearing minerals, such as the quartzites of South Australia, an iron source is less obvious. Assuming these were oxic environments, dissolved iron is unlikely to have been present in the water column in appreciable amounts. It is possible that iron may have been sourced from the interbedded siltstones within the fossil-bearing facies assemblage of the Ediacara Member, rather than from the quartz-rich sands (Gehling, 2000), but further investigation of their mineralogy is required to confirm this. The Ediacara Member was deposited near to the

660 shore, and a local terrestrial freshwater input could feasibly have provided dissolved iron in
661 such environments (e.g., Aller et al., 1986). However in other shallow marine settings (for
662 example the rest of the Rawnsley Quartzite), it is possible that iron availability could have
663 restricted the 'death mask' taphonomic window.

664

665 *Marine sulfate concentrations.*—Marine sulfate concentrations are often stated to have risen
666 throughout the Neoproterozoic, as evidenced by carbon and sulfur isotopic data from South
667 China (McFadden et al., 2008), perhaps due to melting and weathering following the
668 'Snowball' glaciations increasing the sulfate flux to the oceans (Hurtgen et al., 2005;
669 Hurtgen, 2012). Fike and colleagues (2006) record a gradual increase in $\Delta\delta^{34}S$ values from
670 Oman following the Marinoan glacial, indicating a late Neoproterozoic rise in marine sulfate
671 concentrations to levels permitting full expression of bacterial sulfate reduction; a finding
672 corroborated by data from China (Sahoo et al., 2012). In Newfoundland, a notable increase in
673 sulfur isotopic fractionation in sulfides between the Mall Bay and the succeeding Gaskiers
674 and Drook formations has been suggested to indicate an increase in marine sulfate
675 concentrations (Canfield et al., 2007) broadly coincident with the first appearance of
676 macrofossils (upper Drook Formation; Narbonne and Gehling, 2003). However, it remains to
677 be determined whether such increased fractionations are a feature of all Neoproterozoic post-
678 glacial successions (Gorjan et al., 2000).

679 In terms of absolute values, low carbonate associated sulfur (CAS) concentrations,
680 high C_{org}/S_{py} ratios, pyrite values enriched in ^{34}S, and ferruginous deep ocean conditions
681 (Halverson and Hurtgen, 2007; Canfield et al., 2008; Ries et al., 2009), would all appear to
682 suggest that absolute sulfate concentrations in the Ediacaran oceans were lower than those in
683 the Phanerozoic. Direct measurement of sulfate concentrations from late Ediacaran evaporite

684 deposits (e.g., Brennan et al., 2004) is hampered by inconsistency and variability in CAS,
685 barite and phosphate data (summarised in Narbonne et al., 2012). Although $\Delta\delta^{34}S$ values
686 through the Omani Shuram and Buah formations (deposited ~580–550 Ma) appear to reveal
687 evidence for BSR under sulfate limited conditions (Fike et al., 2006), preliminary sulfur
688 isotope data from Newfoundland exhibit values that do not suggest pore-water sulfate became
689 limited at any point in the BSR process (Wacey et al., 2015).

690 In summary, the widespread presence of benthic biofilms on Avalonian seafloors,
691 combined with a terrigenous sedimentation regime characterised by rapid burial of organic
692 matter within densely populated biotic ecosystems, would have created optimal conditions for
693 the microbial breakdown of organic matter by SRB and the production of sulfide ions (cf.,
694 Berner, 1984; Borkow and Babcock, 2003). An increasingly oxic water column, sufficient
695 seawater sulfate to permit BSR, and favourable iron availability in many settings provided
696 suitable chemical conditions to facilitate widespread BSR during this interval, while rapid
697 growth of microbial communities above event beds offered closed-system conditions to limit
698 oxic respiration and support the development of anoxia around buried communities.

699

700 ## Implications for Global Oxygenation

701 Oxygen concentrations in the deep oceans are considered to have undergone a significant
702 increase during the Neoproterozoic (cf., Canfield, 2005; Sahoo et al., 2012; Lyons et al.,
703 2014; Planavsky et al., 2014), the causes of which include elevated burial of organic carbon,
704 increased sedimentation rates, and continental break-up (Knoll et al., 1986; Derry et al., 1992;
705 Kaufman et al., 1997). The timing of this increase, and its relationship to evolutionary events,
706 are widely debated (e.g., Lenton et al., 2014; Sperling et al., 2015). However, it is becoming

increasingly clear that marine redox conditions were not globally stable, and could vary both spatially and temporally during the latest Ediacaran (Li et al., 2015; Wood et al., 2015).

Pyrite burial in sediments can lead to an increase in marine and atmospheric oxygen levels (e.g., Garrells and Perry, 1974), and may also influence nutrient cycling and global climate (Hurtgen, 2012). During the formation of pyrite by sulfate reduction of organic matter, oxygen is liberated via the following pathway (Canfield, 2005):

$$16H^{+} + 8SO_4^{2-} + 2Fe_2O_3 \leftrightarrow 8H_2O + 4FeS_2 + 15O_2$$

In contrast to the Phanerozoic, where oxygen production is dominated by organic carbon burial, it has been calculated that pyrite burial may have been at least as significant a source of oxygen during much of the Proterozoic (Canfield, 2005), although there is uncertainty surrounding the Neoproterozoic due to difficulties in calculating the sulfate flux to the oceans at this time (Canfield, 2004). The observed mineralized veneers in Newfoundland were formed and buried during the late Ediacaran Period, and have only been exposed and oxidised at the surface much more recently. The presence of iron sulfides or their oxidised products on all studied Ediacaran surfaces, sometimes every few centimetres within a stratigraphic section (Supp. Fig. 2C–D), suggests that significant volumes of pyrite were buried globally, in a variety of facies, over the ~40 Myr interval between the first appearance of rangeomorphs at ~580 Ma (Narbonne and Gehling, 2003; Van Kranendonk et al., 2008) and their apparent final occurrence in Namibia close to the Cambrian boundary (Narbonne et al., 1997). Such sedimentary pyrite would be removed from the Earth's surface until its constituent elements were recycled by subduction and hydrothermal circulation or volcanic outgassing, or exhumed and oxidized, all processes that proceed over tens to hundreds of millions of years.

Sedimentary pyrite burial is not widely considered to be a major sink of pyrite in oxic water columns (cf., Canfield, 2004), but the 'closed system' Ediacaran conditions outlined in

this study, whereby laterally extensive pyritization of organic surfaces can occur beneath oxygenated water columns, offer a hitherto unrecognized potential sink of pyrite (with biologically fractionated sulfur isotope compositions) during the latest Neoproterozoic. When coupled with pyrite burial on productive continental margins (i.e., in environments we expect to see pyrite burial), for example in organic rich mudstones from South China where pyrite can reach up to 12% pyrite by weight (McFadden et al., 2008), this 'death mask' pyrite reservoir may have contributed to an increase in marine oxygen concentrations, and thus the gradual oxygenation of the global oceans. This pyrite sink must also be considered in mass balance models of sulfur reservoir volume through geological time, and may help to explain the previously observed imbalance in the Neoproterozoic sulfur cycle (cf., Canfield, 2004). Disruption of matgrounds by motile metazoans may have brought an end to microbially-sealed 'closed-system' conditions in the shallow sub-surface (cf., Seilacher and Pflüger, 1994), and thus to widespread sedimentary pyrite burial in oxic marine settings.

SUMMARY

Framboidal pyrite, and evidence for its oxidation products, is described in association with multiple bedding planes hosting Ediacaran macrofossils in Newfoundland, Canada. Iron sulfides appear to have formed on all surfaces during early diagenesis as a continuous 'veneer', covering the buried seafloors and playing a key role in the replication of fossil morphology. The resultant pyrite is now being oxidized on modern timescales. The presence of pyrite in Newfoundland confirms the applicability of the 'death mask' model of Ediacaran taphonomy (cf., Gehling, 1999) to what has formerly been termed Conception-type preservation (cf., Narbonne, 2005), although it is noted that it is the *presence* of sulfate reducing micro-organisms, and not their formation of laterally continuous microbial mats, which is essential to the process.

Framboidal pyrite veneers at bedding interfaces in Newfoundland supplement observations of pyrite associated with Ediacaran fossils from numerous global localities and disparate facies and lithologies, including carbonates, shales, sandstones and siltstones. The 'death mask' hypothesis may thus be a widely applicable model for soft tissue preservation in the late Ediacaran, importantly explaining the preservation of soft-bodied organisms in coarse-grained sediment. Further experimental work is now required to confirm the precise timescales over which BSR operates, and the types of biological tissue that can be preserved in this way. Finally, the global and persistent burial of sulfides in oxic, siliciclastic basin, shelf and slope settings during the late Ediacaran Period may have contributed to marine oxygenation and ventilation of the oceans prior to the Cambrian Explosion of metazoan diversity.

ACKNOWLEDGEMENTS

The author would like to thank I. Buisman, S. Kearns and B. Buse for SEM and EPMA assistance, J. Stewart and J. Matthews for field assistance, and E. Liu for data processing advice. Discussions with S. Gabbott, R. Gilbaud, A. Page, N. Butterfield, R. Thomas, M. Brasier, D. McIlroy and C. Kenchington have been valuable in preparing this manuscript, and the insightful and constructive reviews and comments of S. Xiao, one anonymous reviewer, and particularly R. Gaines greatly improved the text. This study was supported by a Henslow Junior Research Fellowship from the Cambridge Philosophical Society, and a NERC Independent Research Fellowship [grant number NE/L011409/1]. Sedimentary samples were collected under permits issued by the Government of Newfoundland and Labrador's Parks and Natural Areas Division (for MPER), and Department of Business, Tourism, Culture and Rural Development (for other sites). Readers are advised that access to the MPER Fossil

781 Protection Zone for research is by scientific permit only – contact the Reserve Manager for
782 further information.
783

784 REFERENCES

785 ALLER, R.C., MACKIN, J.E., AND COX, R.T., 1986, Diagenesis of Fe and S in Amazon inner
786 shelf muds: apparent dominance of Fe reduction and implications for the genesis of
787 ironstones: Continental Shelf Research, v. 6, p. 263-289.
788 ALLISON, P.A., AND BRIGGS, D.E.G., 1993, Exceptional fossil record: Distribution of soft-
789 tissue preservation through the Phanerozoic: Geology, v. 21, p. 527-530.
790 ALLISON, P., AND BOTTJER, D., 2011, Taphonomy: Bias and Process Through Time, *in*
791 Allison, P., and Bottjer, D., eds., Taphonomy: Springer, Netherlands, p. 1-17.
792 ANDERSON, E.P., SCHIFFBAUER, J.D., AND XIAO, S., 2011, Taphonomic study of Ediacaran
793 organic-walled fossils confirms the importance of clay minerals and pyrite in Burgess
794 Shale-type preservation: Geology, v. 39, p. 643-646.
795 ANDERSON, M.M., CHOUBERT, G., FAURE-MURET, A., AND TIMOFEIEV, B.V., 1982, Les
796 couches a *Bavlinella* de part et d'autre de l'Atlantique: Bulletin Societe Geologique
797 Francais, v. 2, p. 389-392.
798 BARTELS, C., BRIGGS, D.E.G., AND BRASSEL, G., 1998, Fossils of the Hunsrück Slate: marine
799 life in the Devonian: Cambridge University Press, Cambridge, 309 p.
800 BENGTSON, S., AND ZHAO, Y., 1992, Predatorial borings in Late Precambrian mineralized
801 exoskeletons: Science, v. 257, p. 367-369, doi: 10.1126/science.257.5068.367.
802 BENUS, A.P., 1988, Sedimentological context of a deep-water Ediacaran fauna (Mistaken
803 Point, Avalon Zone, eastern Newfoundland), *in* Landing, E., Narbonne, G.M., and
804 Myrow, P.M., eds., Trace Fossils, Small Shelly Fossils and the Precambrian-

Cambrian Boundary: New York State Museum and Geological Survey Bulletin, p. 8-9.

BERNER, R.A., 1969, Migration of iron and sulfur within anaerobic sediments during early diagenesis: American Journal of Science, v. 267, p. 19-42.

BERNER, R.A., 1970, Sedimentary pyrite formation: American Journal of Science, v. 268, p. 1-23, doi: 10.2475/ajs.268.1.1.

BERNER, R.A., 1984, Sedimentary pyrite formation: An update: Geochimica et Cosmochimica Acta, v. 48, p. 605-615, doi: 10.1016/0016-7037(84)90089-9.

BORKOW, P.S., AND BABCOCK, L.E., 2003, Turning pyrite concretions outside-in: role of biofilms in pyritization of fossils: The Sedimentary Record, v. 1, p. 4-7.

BOTTJER, D.J., HAGADORN, J.W., AND DORNBOS, S.Q., 2000, The Cambrian substrate revolution: GSA Today, v. 10, p. 1-7.

BOUDREAU, B.P., AND WESTRICH, J.T., 1984, The dependence of bacterial sulfate reduction on sulfate concentration in marine sediments: Geochimica et Cosmochimica Acta, v. 48, p. 2503-2516, doi: 10.1016/0016-7037(84)90301-6.

BRASIER, M.D., 2009, Darwin's Lost World. The Hidden History of Animal Life: Oxford University Press, Oxford, 304 p.

BRASIER, M.D., CALLOW, R.H.T., MENON, L.R., AND LIU, A.G., 2010, Osmotrophic Biofilms: From Modern to Ancient, *in* Seckbach, J., and Oren, A., eds., Microbial Mats: Modern and Ancient Microorganisms in Stratified Systems: Springer Science+Business Media B.V., Dordrecht, p. 131-148.

BRASIER, M.D., LIU, A.G., MENON, L.R., MATTHEWS, J.J., MCILROY, D., AND WACEY, D., 2013, Explaining the exceptional preservation of Ediacaran rangeomorphs from Spaniard's Bay, Newfoundland: a hydraulic model: Precambrian Research, v. 231, p. 122-135.

BRENNAN, S.T., LOWENSTEIN, T.K., AND HORITA, J., 2004, Seawater chemistry and the advent of biocalcification: Geology, v. 32, p. 473-476.

BRIGGS, D.E.G., 2003, The role of decay and mineralization in the preservation of soft-bodied fossils: Annual Reviews in Earth and Planetary Sciences, v. 31, p. 275-301.

BRIGGS, D.E.G., BOTTRELL, S.H., AND RAISWELL, R., 1991, Pyritization of soft-bodied fossils: Beecher's Trilobite Bed, Upper Ordovician, New York State: Geology, v. 19, p. 1221-1224, doi: 10.1130/0091-7613(1991)019<1221:posbfb>2.3.co;2.

BRIGGS, D.E.G., RAISWELL, R., BOTTRELL, S.H., HATFIELD, D., AND BARTELS, C., 1996, Controls on the pyritization of exceptionally preserved fossils: an analysis of the Lower Devonian Hunsrück Slate of Germany: American Journal of Science, v. 296, p. 633-663.

BROCK, F., PARKES, R.J., AND BRIGGS, D.E.G., 2006, Experimental pyrite formation associated with decay of plant material: Palaios, v. 21, p. 499-506.

BRUTON, D.L., 1991, Beach and laboratory experiments with the jellyfish *Aurelia* and remarks on some fossil "medusoid" traces, *in* Simonetta, A., and Conway Morris, S., eds., The Early Evolution of Metazoa and the Significance of Problematic Taxa: Cambridge University Press, Cambridge, p. 125-129.

BUATOIS, L.A., NARBONNE, G.M., MÁNGANO, M.G., CARMONA, N.B., AND MYROW, P., 2014, Ediacaran matground ecology persisted into the earliest Cambrian: Nature Communications, v. 5, p. 1-5, doi: 10.1038/ncomms4544.

BUDD, G.E., AND JENSEN, S., 2015, The origin of the animals and a 'Savannah' hypothesis for early bilaterian evolution: Biological Reviews. doi: 10.1111/brv.12239.

BUTLER, I.B., AND RICKARD, D., 2000, Framboidal pyrite formation via the oxidation of iron (II) monosulfide by hydrogen sulphide: Geochimica et Cosmochimica Acta, v. 64, p. 2665-2672, doi: 10.1016/S0016-7037(00)00387-2.

855 BUTTERFIELD, N.J., 2003, Exceptional Fossil Preservation and the Cambrian Explosion:
856 Integrative and Comparative Biology, v. 43, p. 166-177, doi: 10.1093/icb/43.1.166.
857 CAI, Y., AND HUA, H., 2007, Pyritization in the Gaojiashan Biota: Chinese Science Bulletin,
858 v. 52, p. 645-650, doi: 10.1007/s11434-007-0080-9.
859 CAI, Y., SCHIFFBAUER, J.D., HUA, H., AND XIAO, S., 2012, Preservational modes in the
860 Ediacaran Gaojiashan Lagerstätte: Pyritization, aluminosilicification, and
861 carbonaceous compression: Palaeogeography, Palaeoclimatology, Palaeoecology, v.
862 326-328, p. 109-117.
863 CALLOW, R.H.T., AND BRASIER, M.D., 2009, Remarkable preservation of microbial mats in
864 Neoproterozoic siliciclastic settings: Implications for Ediacaran taphonomic models:
865 Earth Science Reviews, v. 96, p. 207-219.
866 CANFIELD, D.E., 2004, The evolution of the Earth surface sulfur reservoir: American Journal
867 of Science, v. 304, p. 839-861.
868 CANFIELD, D.E., 2005, The early history of atmospheric oxygen: Annual Review of Earth and
869 Planetary Sciences, v. 33, p. 1-36.
870 CANFIELD, D.E., AND RAISWELL, R., 1991, Pyrite and fossil preservation, *in* Allison, P.A., and
871 Briggs, D.E.G., eds., Taphonomy: Releasing the data locked in the fossil record:
872 Plenum Press, New York, p. 337-387.
873 CANFIELD, D.E., POULTON, S.W., AND NARBONNE, G.M., 2007, Late-Neoproterozoic deep-
874 ocean oxygenation and the rise of animal life: Science, v. 315, p. 92-95.
875 CANFIELD, D.E., POULTON, S.W., KNOLL, A.H., NARBONNE, G.M., ROSS, G., GOLDBERG, T.,
876 AND STRAUSS, H., 2008, Ferruginous conditions dominated later Neoproterozoic
877 deep-water chemistry: Science, v. 321, p. 949-952.

878 CARBONE, C., AND NARBONNE, G.M., 2014, When life got smart: The evolution of behavioral
879 complexity through the Ediacaran and Early Cambrian of NW Canada: Journal of
880 Paleontology, v. 88, p. 309-330, doi: 10.1666/13-066.
881 CHEN, Z., ZHOU, C., MEYER, M., XIANG, K., SCHIFFBAUER, J.D., YUAN, X., AND XIAO, S.,
882 2013, Trace fossil evidence for Ediacaran bilaterian animals with complex behaviors:
883 Precambrian Research, v. 224, p. 690-701.
884 CHEN, Z., ZHOU, C., XIAO, S., WANG, W., GUAN, C., HUA, H., AND YUAN, X., 2014, New
885 Ediacara fossils preserved in marine limestone and their ecological implications:
886 Scientific Reports, v. 4, p. 4180, doi: 10.1038/srep04180.
887 CLAPHAM, M.E., NARBONNE, G.M., AND GEHLING, J.G., 2003, Paleoecology of the oldest
888 known animal communities: Ediacaran assemblages at Mistaken Point,
889 Newfoundland: Paleobiology, v. 29, p. 527-544.
890 COCKS, L.R.M., MCKERROW, W.S., AND VAN STAAL, C.R., 1997, The margins of Avalonia:
891 Geological Magazine, v. 134, p. 627-636.
892 DARROCH, S.A.F., LAFLAMME, M., SCHIFFBAUER, J.D., AND BRIGGS, D.E.G., 2012,
893 Experimental formation of a microbial death mask: PALAIOS, v. 27, p. 293-303.
894 DARROCH, S.A., LAFLAMME, M., AND CLAPHAM, M.E., 2013, Population structure of the
895 oldest known macroscopic communities from Mistaken Point, Newfoundland:
896 Paleobiology, v. 39, p. 591-608.
897 DARROCH, S.A.F., SPERLING, E.A., BOAG, T.H., RACICOT, R.A., MASON, S.J., MORGAN, A.S.,
898 TWEEDT, S., MYROW, P., JOHNSTON, D.T., ERWIN, D.H., AND LAFLAMME, M., 2015,
899 Biotic replacement and mass extinction of the Ediacara biota: Proceedings of the
900 Royal Society of London B: Biological Sciences, v. 282, doi:
901 10.1098/rspb.2015.1003.

902 DERRY, L.A., KAUFMAN, A.J., AND JACOBSEN, S.B., 1992, Sedimentary cycling and
903 environmental change in the late Proterozoic: evidence from stable and radiogenic
904 isotopes: Geochimica et Cosmochimica Acta, v. 56, p. 1317-1329.
905 DONALD, R., AND SOUTHAM, G., 1999, Low temperature anaerobic bacterial diagenesis of
906 ferrous monosulfide to pyrite: Geochimica et Cosmochimica Acta, v. 63, p. 2019-
907 2023, doi: 10.1016/S0016-7037(99)00140-4.
908 DOS REIS, M., THAWORNWATTANA, Y., ANGELIS, K., TELFORD, M.J., DONOGHUE, P.C.J., AND
909 YANG, Z., 2015, Uncertainty in the timing of origin of animals and the limits of
910 precision in molecular timescales: Current Biology, v. 25, p. 2939-2950, doi:
911 10.1016/j.cub.2015.09.066.
912 DORNBOS, S.Q., BOTTJER, D.J., AND CHEN, J.Y., 2004, Evidence for seafloor microbial mats
913 and associated metazoan lifestyles in Lower Cambrian phosphorites of Southwest
914 China: Lethaia, v. 37, p. 127-137.
915 DROSER, M.L., AND GEHLING, J.G., 2015, The advent of animals: The view from the
916 Ediacaran: Proceedings of the National Academy of Sciences, v. 112, p. 4865-4870,
917 doi: 10.1073/pnas.1403669112.
918 DROSER, M.L., GEHLING, J.G., AND JENSEN, S.R., 2006, Assemblage palaeoecology of the
919 Ediacara biota: The unabridged edition?: Palaeogeography, Palaeoclimatology,
920 Palaeoecology, v. 232, p. 131-147.
921 DUGGEN, S., OLGUN, N., HOFFMAN, L., DIETZE, H., DELMELLE, P., AND TESCHNER, C., 2010,
922 The role of airborne volcanic ash for the surface ocean biogeochemical iron-cycle: A
923 review: Biogeosciences, v. 7, p. 827–844.
924 DZIK, J., 2003, Anatomical information content in the Ediacaran fossils and their possible
925 zoological affinities: Integrative and Comparative Biology, v. 43, p. 114-126.

926 DZIK, J., AND MARTYSHYN, A., 2015, Taphonomy of the Ediacaran *Podolimirus* and
927 associated dipleurozoans from the Vendian of Ukraine: Precambrian Research, v. 269,
928 p. 139-146, doi: 10.1016/j.precamres.2015.08.015.
929 ERWIN, D.H., LAFLAMME, M., TWEEDT, S.M., SPERLING, E.A., PISANI, D., AND PETERSON,
930 K.J., 2011, The Cambrian Conundrum: Early divergence and later ecological success
931 in the early history of animals: Science, v. 334, p. 1091-1097.
932 FARRELL, Ú.C., MARTIN, M.J., HAGADORN, J.W., WHITELEY, T., AND BRIGGS, D.E.G., 2009,
933 Beyond Beecher's Trilobite Bed: Widespread pyritization of soft tissues in the Late
934 Ordovician Taconic foreland basin: Geology, v. 37, p. 907-910, doi:
935 10.1130/g30177a.1.
936 FARRELL, Ú.C., BRIGGS, D.E.G., HAMMARLUND, E.U., SPERLING, E.A., AND GAINES, R.R.,
937 2013, Paleoredox and pyritization of soft-bodied fossils in the Ordovician Frankfort
938 Shale of New York: American Journal of Science, v. 313, p. 452-489, doi:
939 10.2475/05.2013.02.
940 FEDONKIN, M.A., 1985, Precambrian metazoans: the problems of preservation, systematics
941 and evolution [and discussion]: Philosophical Transactions of the Royal Society,
942 London, Series B, v. 311, p. 27-45.
943 FEDONKIN, M.A., AND WAGGONER, B.M., 1997, The Late Precambrian fossil *Kimberella* is a
944 mollusc-like bilaterian organism: Nature, v. 388, p. 868-871.
945 FEDONKIN, M.A., GEHLING, J.G., GREY, K., NARBONNE, G.M., AND VICKERS-RICH, P., 2007,
946 The rise of animals: Evolution and diversification of the Kingdom Animalia: John
947 Hopkins University Press, Baltimore, 326 p.
948 FIKE, D.A., GROTZINGER, J.P., PRATT, L.M., AND SUMMONS, R.E., 2006, Oxidation of the
949 Ediacaran Ocean: Nature, v. 444, p. 744-747.

950 GABBOTT, S.E., XIAN-GUANG, H., NORRY, M.J., AND SIVETER, D.J., 2004, Preservation of
951 Early Cambrian animals of the Chengjiang biota: Geology, v. 32, p. 901-904, doi:
952 10.1130/g20640.1.
953 GAINES, R.R., HAMMARLUND, E.U., HOU, X., QI, C., GABBOTT, S.E., ZHAO, Y., PENG, J., AND
954 CANFIELD, D.E., 2012a, Mechanism for Burgess Shale-type preservation: Proceedings
955 of the National Academy of Sciences, v. 109, p. 5180-5184.
956 GAINES, R.R., BRIGGS, D.E.G., ORR, P.J., AND VAN ROY, P., 2012b, Preservation of giant
957 anomalocaridids in silica-chlorite concretions from the Early Ordovician of Morocco:
958 PALAIOS, v. 27, p. 317-325.
959 GARRELLS, R.M., AND PERRY JR., E.A., 1974, Cycling of carbon, sulfur, and oxygen through
960 geologic time, *in* Goldberg, E.D., ed., The Sea: John Wiley and Sons, New York, p.
961 303-336.
962 GEHLING, J.G., 1999, Microbial mats in terminal Proterozoic siliciclastics: Ediacaran death
963 masks: PALAIOS, v. 14, p. 40-57.
964 GEHLING, J.G., 2000, Environmental interpretation and a sequence stratigraphic framework
965 for the terminal Proterozoic Ediacara Member within the Rawnsley Quartzite, South
966 Australia: Precambrian Research, v. 100, p. 65-95.
967 GEHLING, J.G., AND NARBONNE, G.M., 2007, Spindle-shaped Ediacara fossils from the
968 Mistaken Point assemblage, Avalon Zone, Newfoundland: Canadian Journal of Earth
969 Sciences, v. 44, p. 367-387.
970 GEHLING, J.G., DROSER, M.L., JENSEN, S.R., AND RUNNEGAR, B.N., 2005, Ediacaran
971 organisms: relating form and function, *in* Briggs, D.E.G., ed., Evolving form and
972 function: fossils and development: proceedings of a symposium honoring Adolf
973 Seilacher for his contributions to paleontology, in celebration of his 80th birthday:
974 Yale University, New Haven, Conn., p. 43-67.

975 GLAESSNER, M.F., AND WADE, M., 1966, The Late Precambrian fossils from Ediacara, South
976 Australia: Palaeontology, v. 9, p. 599-628.
977 GOLDHABER, M.B., AND KAPLAN, I.R., 1974, The sulfur cycle, *in* Goldberg, E.D., ed., The
978 Sea: Wiley-Interscience, New York, v. 5, p. 569-655.
979 GORJAN, P., VEEVERS, J.J., AND WALTER, M.R., 2000, Neoproterozoic sulfur-isotope variation
980 in Australia and global implications: Precambrian Research, v. 100, p. 151-179, doi:
981 10.1016/S0301-9268(99)00073-X.
982 GRAZHDANKIN, D.V., 2003, Structure and depositional environment of the Vendian complex
983 in the southeastern White Sea area: Stratigraphy and Geological Correlation, v. 11, p.
984 313-331.
985 GRAZHDANKIN, D., 2004, Patterns of distribution in the Ediacaran biotas: facies versus
986 biogeography and evolution: Paleobiology, v. 30, p. 203-221.
987 GRAZHDANKIN, D.V., AND SEILACHER, A., 2005, A re-examination of the Nama-type Vendian
988 organism *Rangea schneiderhoehni*: Geological Magazine, v. 142, p. 571-582.
989 GRAZHDANKIN, D., AND GERDES, G., 2007, Ediacaran microbial colonies: Lethaia, v. 40, p.
990 201-210.
991 GRAZHDANKIN, D., BALTHASAR, U., NAGOVITSIN, K.E., AND KOCHNEV, B.B., 2008,
992 Carbonate-hosted Avalon-type fossils in arctic Siberia: Geology, v. 36, p. 803-806.
993 GREY, K., AND WILLMAN, S., 2009, Taphonomy of Ediacaran acritarchs from Australia:
994 significance for taxonomy and biostratigraphy: PALAIOS, v. 24, p. 239-256, doi:
995 10.2110/palo.2008.p08-020r.
996 GRIMES, S.T., BROCK, F., RICKARD, D., DAVIES, K.L., EDWARDS, D., BRIGGS, D.E.G., AND
997 PARKES, R.J., 2001, Understanding fossilization: experimental pyritization of plants:
998 Geology, v. 29, p. 123-126.

GRIMES, S.T., DAVIES, K.L., BUTLER, I.B., BROCK, F., EDWARDS, D., RICKARD, D., BRIGGS, D.E.G., AND PARKES, R.J., 2002, Fossil plants from the Eocene London Clay: the use of pyrite textures to determine the mechanism of pyritization: Journal of the Geological Society, v. 159, p. 493-501.

GUILBAUD, R., POULTON, S.W., BUTTERFIELD, N.J., ZHU, M., AND SHIELDS-ZHOU, G.A., 2015, A global transition to ferruginous conditions in the early Neoproterozoic oceans: Nature Geoscience, v. 8, p. 466-470, doi: 10.1038/ngeo2434

HALL, M., KAUFMAN, A.J., VICKERS-RICH, P., IVANTSOV, A., TRUSLER, P., LINNEMANN, U., HOFMANN, M., ELLIOTT, D., CUI, H., FEDONKIN, M., HOFFMANN, K.-H., WILSON, S.A., SCHNEIDER, G., AND SMITH, J., 2013, Stratigraphy, palaeontology and geochemistry of the late Neoproterozoic Aar Member, southwest Namibia: Reflecting environmental controls on Ediacara fossil preservation during the terminal Proterozoic in African Gondwana: Precambrian Research, v. 238, p. 214-232, doi: 10.1016/j.precamres.2013.09.009.

HALVERSON, G.P., AND HURTGEN, M.T., 2007, Ediacaran growth of the marine sulfate reservoir: Earth and Planetary Science Letters, v. 263, p. 32-44.

HALVERSON, G.P., HURTGEN, M.T., PORTER, S.M., AND COLLINS, A.S., 2009, Chapter 10 Neoproterozoic-Cambrian biogeochemical evolution, *in* Gaucher, C., Sial, A.N., Frimmel, H.E. and Halverson, G.P., eds., Developments in Precambrian Geology: Elsevier, p. 351-365.

HOFMANN, H.J., HILL, J., AND KING, A.F., 1979, Late Precambrian microfossils, southeastern Newfoundland: Current Research, Part B, Geological Survey of Canada, v. 79-1B, p. 83-98.

HOFMANN, H.J., O'BRIEN, S.J., AND KING, A.F., 2008, Ediacaran biota on Bonavista Peninsula, Newfoundland, Canada: Journal of Paleontology, v. 82, p. 1-36.

1024 HUDSON, J.D., 1982, Pyrite in ammonite-bearing shales from the Jurassic of England and
1025 Germany: Sedimentology, v. 29, p. 639-667, doi: 10.1111/j.1365-
1026 3091.1982.tb00072.x.
1027 HURTGEN, M.T., 2012, The marine sulfur cycle, revisited: Science, v. 337, p. 305-306.
1028 HURTGEN, M.T., ARTHUR, M.A., AND HALVERSON, G.P., 2005, Neoproterozoic sulfur
1029 isotopes, the evolution of microbial sulfur species, and the burial efficiency of sulfide
1030 as sedimentary pyrite: Geology, v. 33, p. 41-44, doi: 10.1130/g20923.1.
1031 ICHASO, A.A., DALRYMPLE, R.W., AND NARBONNE, G.M., 2007, Paleoenvironmental and
1032 basin analysis of the late Neoproterozoic (Ediacaran) upper Conception and St. John's
1033 groups, west Conception Bay, Newfoundland: Canadian Journal of Earth Sciences, v.
1034 44, p. 25-41.
1035 INTERNATIONAL NETWORK FOR ACID PREVENTION, 2014, Global Acid Rock Drainage Guide:
1036 http://www.gardguide.com/images/5/5f/TheGlobalAcidRockDrainageGuide.pdf
1037 IVANTSOV, A. YU., 2016, Reconstruction of *Charniodiscus yorgensis* (Macrobiota from the
1038 Vendian of the White Sea): Paleontological Journal, v. 50, p. 1-12.
1039 JENKINS, R.J.F., 1992, Functional and ecological aspects of Ediacaran assemblages, *in* Lipps,
1040 J.H., and Signor, P.W., eds., Origin and Early Evolution of the Metazoa: Plenum,
1041 New York/London, p. 131-176.
1042 JIANG, G., SHI, X., ZHANG, S., WANG, Y., AND XIAO, S., 2011, Stratigraphy and
1043 paleogeography of the Ediacaran Doushantuo Formation (ca. 635-551 Ma) in south
1044 China: Gondwana Research, v. 19, p. 831-849.
1045 JØRGENSEN, B.B., 1977, Bacterial sulfate reduction within reduced microniches of oxidized
1046 marine sediments: Marine Biology, v. 41, p. 7-17.

KAUFMAN, A.J., KNOLL, A.H., AND NARBONNE, G.M., 1997, Isotopes, ice ages and terminal Proterozoic Earth history: Proceedings of the National Academy of Sciences, USA, v. 94, p. 6600-6605.

KENCHINGTON, C.G., AND WILBY, P.R., 2015, Of time and taphonomy: preservation in the Ediacaran, *in* Laflamme, M., Schiffbauer, J.D., and Darroch, S.A.F., eds., Reading and writing of the fossil record: Preservational pathways to exceptional preservation: The Paleontological Society Papers, v. 20, p. 101-122.

KIIPLI, T., KIIPLI, E., KALLASTE, T., HINTS, R., SOMELAR, P., AND KIRSIMÄE, K., 2007, Altered volcanic ash as an indicator of marine environment, reflecting pH and sedimentation rate – example from the Ordovician Kinnekulle bed of Baltoscandia: Clays and Clay Minerals, v. 55, p. 177-188, doi: 10.1346/ccmn.2007.0550207.

KNOLL, A.H., HAYES, J.M., KAUFMAN, A.J., SWETT, K., AND LAMBERT, I.B., 1986, Secular variation in carbon isotope ratios from Upper Proterozoic successions of Svalbard and east Greenland: Nature, v. 321, p. 832-838.

LAFLAMME, M., NARBONNE, G.M., AND ANDERSON, M.M., 2004, Morphometric analysis of the Ediacaran frond *Charniodiscus* from the Mistaken Point Formation, Newfoundland: Journal of Paleontology, v. 78, p. 827-837.

LAFLAMME, M., SCHIFFBAUER, J.D., NARBONNE, G.M., AND BRIGGS, D.E.G., 2011, Microbial biofilms and the preservation of the Ediacara biota: Lethaia, v. 44, p. 203-213, doi: 10.1111/j.1502-3931.2010.00235.x.

LAFLAMME, M., DARROCH, S.A.F., TWEEDT, S.M., PETERSON, K.J., AND ERWIN, D.H., 2013, The end of the Ediacara biota: Extinction, biotic replacement, or Cheshire Cat?: Gondwana Research, v. 23, p. 558-573.

LANDING, E., NARBONNE, G.M., MYROW, P.M., AND MATTHEW, G.F., 1988, Trace fossils, small shelly fossils and the Precambrian-Cambrian boundary: University of the State

of New York, New York State Museum/Geological Survey, State Education Department, 81 p.

LEAVITT, W.D., HALEVY, I., BRADLEY, A.S., AND JOHNSTON, D.T., 2013, Influence of sulfate reduction rates on the Phanerozoic sulfur isotope record: Proceedings of the National Academy of Sciences, v. 110, p. 11244-11249, doi: 10.1073/pnas.1218874110.

LENTON, T.M., BOYLE, R.A., POULTON, S.W., SHIELDS-ZHOU, G.A., AND BUTTERFIELD, N.J., 2014, Co-evolution of eukaryotes and ocean oxygenation in the Neoproterozoic era: Nature Geoscience, v. 7, p. 257-265, doi: 10.1038/ngeo2108.

LI, C., LOVE, G.D., LYONS, T.W., FIKE, D.A., SESSIONS, A.L., AND CHU, X., 2010, A stratified redox model for the Ediacaran ocean: Science, v. 328, p. 80-83.

LI, C., PLANAVSKY, N.J., SHI, W., ZHANG, Z., ZHOU, C., CHENG, M., TARHAN, L.G., LUO, G., AND XIE, S., 2015, Ediacaran marine redox heterogeneity and early animal ecosystems: Scientific Reports, v. 5, p. 17097, doi: 10.1038/srep17097.

LIU, A.G., MCILROY, D., AND BRASIER, M.D., 2010, First evidence for locomotion in the Ediacara biota from the 565Ma Mistaken Point Formation, Newfoundland: Geology, v. 38, p. 123-126.

LIU, A.G., MCILROY, D., ANTCLIFFE, J.B., AND BRASIER, M.D., 2011, Effaced preservation in the Ediacaran biota of Avalonia and its implications for the early macrofossil record: Palaeontology, v. 54, p. 607-630.

LIU, A.G., MATTHEWS, J.J., MENON, L.R., MCILROY, D., AND BRASIER, M.D., 2014*a*, *Haootia quadriformis* n. gen., n. sp., interpreted as a muscular cnidarian impression from the Late Ediacaran period (approx. 560 Ma): Proceedings of the Royal Society B: Biological Sciences, v. 281, p. 20141202, doi: 10.1098/rspb.2014.1202.

LIU, A.G., MCILROY, D., MATTHEWS, J.J., AND BRASIER, M.D., 2014*b*, Confirming the metazoan character of a 565 Ma trace-fossil assemblage from Mistaken Point, Newfoundland: PALAIOS, v. 29, p. 420-430.

LIU, A.G., KENCHINGTON, C.G., AND MITCHELL, E.G., 2015, Remarkable insights into the paleoecology of the Avalonian Ediacaran macrobiota: Gondwana Research, v. 27, p. 1355-1380, doi: 10.1016/j.gr.2014.11.002.

LIU, A.G., MATTHEWS, J.J., AND MCILROY, D., 2016, The *Beothukis*/*Culmofrons* problem and its bearing on Ediacaran macrofossil taxonomy: evidence from an exceptional new fossil locality: Palaeontology, v. 59, p. 45-58.

LOWSON, R.T., 1982, Aqueous oxidation of pyrite by molecular oxygen: Chemical Reviews, v. 82, p. 461-497, doi: 10.1021/cr00051a001.

LYONS, T.W., ANBAR, A.D., SEVERMANN, S., SCOTT, C., AND GILL, B.C., 2009, Tracking euxinia in the ancient ocean: A multiproxy perspective and Proterozoic case study: Annual Review of Earth and Planetary Sciences, v. 37, p. 507-534.

LYONS, T.W., REINHARD, C.T., AND PLANAVSKY, N.J., 2014, The rise of oxygen in Earth's early ocean and atmosphere: Nature, v. 506, p. 307-315, doi: 10.1038/nature13068.

MACLEAN, L.C.W., TYLISZCZAK, T., GILBERT, P.U.P.A., ZHOU, D., PRAY, T.J., ONSTOTT, T.C., AND SOUTHAM, G., 2008, A high-resolution chemical and structural study of framboidal pyrite formed within a low-temperature bacterial biofilm: Geobiology, v. 6, p. 471-480.

MÁNGANO, M.G., AND BUATOIS, L.A., 2014, Decoupling of body-plan diversification and ecological structuring during the Ediacaran–Cambrian transition: evolutionary and geobiological feedbacks: Proceedings of the Royal Society B: Biological Sciences, v. 281, doi: 10.1098/rspb.2014.0038.

1119 MAPSTONE, N.B., AND MCILROY, D., 2006, Ediacaran fossil preservation: Taphonomy and
1120 diagenesis of a discoid biota from the Amadeus Basin, central Australia: Precambrian
1121 Research, v. 149, p. 126-148.
1122 MARTILL, D., 1998, Resolution of the fossil record: the fidelity of preservation, *in* Donovan,
1123 S.K., and Paul, C.R.C., eds., The adequacy of the fossil record: London, Wiley, p. 55-
1124 74.
1125 MASON, S.J., NARBONNE, G.M., DALRYMPLE, R.W., AND O'BRIEN, S.J., 2013,
1126 Paleoenvironmental analysis of Ediacaran strata in the Catalina Dome, Bonavista
1127 Peninsula, Newfoundland: Canadian Journal of Earth Sciences, v. 50, p. 197-212.
1128 MCFADDEN, K.A., HUANG, J., CHU, X., JIANG, G., KAUFMAN, A.J., ZHOU, C., YUAN, X., AND
1129 XIAO, S., 2008, Pulsed oxidation and biological evolution in the Ediacaran
1130 Doushantuo Formation: Proceedings of the National Academy of Sciences, USA, v.
1131 105, p. 3197-3202.
1132 MCILROY, D., CRIMES, T.P., AND PAULEY, J.C., 2005, Fossils and matgrounds from the
1133 Neoproterozoic Longmyndian Supergroup, Shropshire, U.K.: Geological Magazine,
1134 v. 142, p. 441-455.
1135 MENON, L.R., MCILROY, D., LIU, A.G., AND BRASIER, M.D., 2016, The dynamic influence of
1136 microbial mats on sediments: fluid escape and pseudofossil formation in the
1137 Ediacaran Longmyndian Supergroup, UK: Journal of the Geological Society, London,
1138 v. 173, p. 177-185. doi: 10.1144/jgs2015-036.
1139 MEYER, M., ELLIOTT, D., SCHIFFBAUER, J.D., HALL, M., HOFFMAN, K.H., SCHNEIDER, G.,
1140 VICKERS-RICH, P., AND XIAO, S., 2014*a*, Taphonomy of the Ediacaran fossil
1141 *Pteridinium simplex* preserved three-dimensionally in mass flow deposits, Nama
1142 Group, Namibia: Journal of Paleontology, v. 88, p. 240-252, doi: 10.1666/13-047.

1143 MEYER, M., XIAO, S., GILL, B.C., SCHIFFBAUER, J.D., CHEN, Z., ZHOU, C., AND YUAN, X.,
1144 2014*b*, Interactions between Ediacaran animals and microbial mats: insights from
1145 *Lamonte trevallis*, a new trace fossil from the Dengying Formation of South China:
1146 Palaeogeography, Palaeoclimatology, Palaeoecology, v. 396, p. 62-74.
1147 MOCZYDŁOWSKA, M., WESTALL, F., AND FOUCHER, F., 2014, Microstructure and
1148 biogeochemistry of the organically preserved Ediacaran metazoan *Sabellidites*:
1149 Journal of Paleontology, v. 88, p. 224-239, doi: doi:10.1666/13-003.
1150 MOORE, R.A., AND LIEBERMAN, B.S., 2009, Preservation of early and Middle Cambrian soft-
1151 bodied arthropods from the Pioche Shale, Nevada, USA: Palaeogeography,
1152 Palaeoclimatology, Palaeoecology, v. 277, p. 57-62, doi:
1153 10.1016/j.palaeo.2009.02.014.
1154 MYROW, P.M., 1995, Neoproterozoic rocks of the Newfoundland Avalon Zone: Precambrian
1155 Research, v. 73, p. 123-136, doi: 10.1016/0301-9268(94)00074-2.
1156 NARBONNE, G.M., 2004, Modular construction in the Ediacaran biota: Science, v. 305, p.
1157 1141-1144.
1158 NARBONNE, G.M., 2005, The Ediacara Biota: Neoproterozoic origin of animals and their
1159 ecosystems: Annual Reviews in Earth and Planetary Sciences, v. 33, p. 421-442.
1160 NARBONNE, G.M., AND GEHLING, J.G., 2003, Life after snowball: the oldest complex
1161 Ediacaran fossils: Geology, v. 31, p. 27-30.
1162 NARBONNE, G.M., SAYLOR, B.Z., AND GROTZINGER, J.P., 1997, The youngest Ediacaran
1163 fossils from southern Africa: Journal of Paleontology, v. 71, p. 953-967.
1164 NARBONNE, G.M., DALRYMPLE, R.W., LAFLAMME, M., GEHLING, J.G., AND BOYCE, W.D.,
1165 2005, Life after Snowball: Mistaken Point Biota and the Cambrian of the Avalon:
1166 North American Paleontological Convention Field Trip Guidebook, Halifax, Nova
1167 Scotia, 98 p.

1168 NARBONNE, G.M., XIAO, S., AND SHIELDS, G.A., 2012, The Ediacaran Period, *in* Gradstein,
1169 F.M., Ogg, J.G., Schmitz, M.D., and Ogg, G., eds., The Geologic Time Scale 2012:
1170 Elsevier, Amsterdam, p. 413-435.
1171 NARBONNE, G.M., LAFLAMME, M., TRUSLER, P.W., DALRYMPLE, R.W., AND GREENTREE, C.,
1172 2014, Deep-water Ediacaran fossils from northwestern Canada: taphonomy, ecology,
1173 and evolution: Journal of Paleontology, v. 88, p. 207-223.
1174 NORRIS, R.D., 1989, Cnidarian taphonomy and affinities of the Ediacara biota: Lethaia, v. 22,
1175 p. 381-393.
1176 O'BRIEN, S.J., AND KING, A.F., 2005, Late Neoproterozoic (Ediacaran) stratigraphy of the
1177 Avalon zone sedimentary rocks, Bonavista Peninsula, Newfoundland: Current
1178 Research, Newfoundland and Labrador Department of Natural Resources Geological
1179 Survey, v. 05-1, p. 101-113.
1180 ORR, P.J., BENTON, M.J., AND BRIGGS, D.E.G., 2003, Post-Cambrian closure of the deep-
1181 water slope-basin taphonomic window: Geology, v. 31, p. 769-772, doi:
1182 10.1130/g19193.1.
1183 PAGE, A., GABBOTT, S.E., WILBY, P.R., AND ZALASIEWICZ, J.A., 2008, Ubiquitous Burgess
1184 Shale–style "clay templates" in low-grade metamorphic mudrocks: Geology, v. 36, p.
1185 855-858, doi: 10.1130/g24991a.1.
1186 PAPEZIK, V.S., 1974, Prehnite-pumpellyite facies metamorphism of late Precambrian rocks of
1187 the Avalon Peninsula, Newfoundland: Canadian Mineralogist, v. 12, p. 463-468.
1188 PFLUG, H.D., 1972, Systematik der jung-präkambrischen Petalonamae Pflug 1970:
1189 Paläontologische Zeitschrift, v. 46, p. 56-67.
1190 PLANAVSKY, N.J., REINHARD, C.T., WANG, X., THOMSON, D., MCGOLDRICK, P., RAINBIRD,
1191 R.H., JOHNSON, T., FISCHER, W.W., AND LYONS, T.W., 2014, Low Mid-Proterozoic

atmospheric oxygen levels and the delayed rise of animals: Science, v. 346, p. 635-638, doi: 10.1126/science.1258410.

POPA, R., KINKLE, B.K., AND BADESCU, A., 2004, Pyrite framboids as biomarkers for iron-sulfur systems: Geomicrobiology Journal, v. 21, p. 193-206.

RAISWELL, R., 1982, Pyrite texture, isotopic composition and the availability of iron: American Journal of Science, v. 282, p. 1244-1263, doi: 10.2475/ajs.282.8.1244.

RAISWELL, R., WHALER, K., DEAN, S., COLEMAN, M.L., AND BRIGGS, D.E.G., 1993, A simple three-dimensional model of diffusion-with-precipitation applied to localised pyrite formation in framboids, fossils and detrital iron minerals: Marine Geology, v. 113, p. 89-100, doi: 10.1016/0025-3227(93)90151-K.

RETALLACK, G., 2014, Volcanosedimentary paleoenvironments of Ediacaran fossils in Newfoundland: Geological Society of America Bulletin, v. 126, p. 619-638.

RICKARD, D., 2012, Sulfidic sediments and sedimentary rocks: Elsevier, 801 p.

RIES, J.B., FIKE, D.A., PRATT, L.M., LYONS, T.W., AND GROTZINGER, J.P., 2009, Superheavy pyrite ($\delta^{34}Spyr > \delta^{34}S_{CAS}$) in the terminal Proterozoic Nama Group, southern Namibia: A consequence of low seawater sulfate at the dawn of animal life: Geology, v. 37, p. 743-746, doi: 10.1130/g25775a.1.

RIMSTIDT, J.D., AND VAUGHAN, D.J., 2003, Pyrite oxidation: a state-of-the-art assessment of the reaction mechanism: Geochimica et Cosmochimica Acta, v. 67, p. 873-880, doi: 10.1016/S0016-7037(02)01165-1.

ROGOV, V., MARUSIN, V., BYKOVA, N., GOY, Y., NAGOVITSIN, K.E., KOCHNEV, B., KARLOVA, G.A., AND GRAZHDANKIN, D., 2012, The oldest evidence of bioturbation on Earth: Geology, v. 40, p. 395-398.

ROWLAND, S.M., AND RODRIGUEZ, M.G., 2014, A multicellular alga with exceptional preservation from the Ediacaran of Nevada: Journal of Paleontology, v. 88, p. 263-268, doi: 10.1666/13-075.

SAHOO, S.K., PLANAVSKY, N.J., KENDALL, B., WANG, X., SHI, X., SCOTT, C., ANBAR, A.D., LYONS, T.W., AND JIANG, G., 2012, Ocean oxygenation in the wake of the Marinoan glaciation: Nature, v. 489, p. 546-549.

SARIA, L., SHIMAOKA, T., AND MIYAWAKI, K., 2006, Leaching of heavy metals in acid mine drainage: Waste Management & Research, v. 24, p. 134-140.

SCHALLREUTER, R., 1984, Framboidal pyrite in deep-sea sediments: Initial Reports of the Deep Sea Drilling Project, v. 75, p. 875-891.

SCHIFFBAUER, J.D., AND LAFLAMME, M., 2012, Lagerstätten through time: a collection of exceptional preservational pathways from the terminal Neoproterozoic through today: PALAIOS, v. 27, p. 275-278.

SCHIFFBAUER, J.D., XIAO, S., CAI, Y., WALLACE, A.F., HUA, H., HUNTER, J., XU, H., PENG, Y., AND KAUFMAN, A.J., 2014, A unifying model for Neoproterozoic–Palaeozoic exceptional fossil preservation through pyritization and carbonaceous compression: Nature Communications, v. 5, no. 5754, doi: 10.1038/ncomms6754.

SEILACHER, A., 1992, Vendobionta and Psammocorallia: lost constructions of Precambrian evolution: Journal of the Geological Society, London, v. 149, p. 607-613.

SEILACHER, A., AND PFLÜGER, F., 1994, From biomats to benthic agriculture: A biohistoric revolution, *in* Krumbein, W.E., Peterson, D.M., and Stal, L.J., eds., Biostabilization of Sediments: Bibliotheks-und Informationssystem der Carl von Ossietzky Universität Odenburg, p. 97-105.

SEILACHER, A., REIF, W.-E., WESTPHAL, F., RIDING, R., CLARKSON, E.N.K., AND WHITTINGTON, H.B., 1985, Sedimentological, ecological and temporal patterns of

fossil Lagerstätten [and Discussion]: Philosophical Transactions of the Royal Society, London, v. 311, p. 5-24, doi: 10.1098/rstb.1985.0134.

SEREZHNIKOVA, E., 2011, Microbial binding as a probable cause of taphonomic variability of Vendian fossils: carbonate casting?, *in* Reitner, J., Queric, N.V., and Arp, G., eds., Advances in Stromatolite Geobiology: Springer, Berlin Heidelberg, p. 525-535.

SPERLING, E.A., 2013, Tackling the 99%; Can we begin to understand the paleoecology of the small and soft-bodied animal majority: The Paleontological Society Papers, v. 19, p. 77-86.

SPERLING, E.A., WOLOCK, C.J., MORGAN, A.S., GILL, B.C., KUNZMANN, M., HALVERSON, G.P., MACDONALD, F.A., KNOLL, A.H., AND JOHNSTON, D.T., 2015, Statistical analysis of iron geochemical data suggests limited late Proterozoic oxygenation: Nature, v. 523, p. 451-454, doi: 10.1038/nature14589

STEINER, M., AND REITNER, J., 2001, Evidence of organic structures in Ediacara-type fossils and associated microbial mats: Geology, v. 29, p. 1119-1122.

STUMM, W., AND MORGAN, J.J., 1981, Aquatic chemistry: an introduction emphasizing chemical equilibria in natural waters: John Wiley, New York, 795 p.

SWEENEY, R.E., AND KAPLAN, I.R., 1973, Pyrite framboid formation: laboratory synthesis and marine sediments: Economic Geology, v. 68, p. 618-634.

TARHAN, L.G., DROSER, M.L., PLANAVSKY, N.J., AND JOHNSTON, D.T., 2015, Protracted development of bioturbation through the early Palaeozoic Era: Nature Geoscience, v. 8, p. 865-869.

TIMOFEYEV, B.V., CHOUBERT, G., AND FAURE-MURET, A., 1980, Acritarchs of the Precambrian in mobile zones: Earth Science Reviews, v. 16, p. 249-255.

VAN KRANENDONK, M.J., GEHLING, J.G., AND SHIELDS, G.A., 2008, Precambrian, *in* Ogg, J.G., Ogg, G., and Gradstein, F.M., eds., The Concise Geologic Time Scale: Cambridge University Press, Cambridge, p. 23-36.

VICKERS-RICH, P., IVANTSOV, A.Y., TRUSLER, P.W., NARBONNE, G.M., HALL, M., WILSON, S.A., GREENTREE, C., FEDONKIN, M.A., ELLIOTT, D.A., HOFFMANN, K.-H., AND SCHNEIDER, G.I.C., 2013, Reconstructing *Rangea*: New discoveries from the Ediacaran of southern Namibia: Journal of Paleontology, v. 87, p. 1-15.

WACEY, D., KILBURN, M.R., SAUNDERS, M., CLIFF, J.B., KONG, C., LIU, A.G., MATTHEWS, J.J., AND BRASIER, M.D., 2015, Uncovering framboidal pyrite biogenicity using nano-scale CN_{org} mapping: Geology, v. 43, p. 27-30, doi: 10.1130/g36048.1.

WADE, M., 1968, Preservation of soft-bodied animals in Precambrian sandstones at Ediacara, South Australia: Lethaia, v. 1, p. 238-267.

WANG, W., GUAN, C., ZHOU, C., WAN, B., TANG, Q., CHEN, X., CHEN, Z., AND YUAN, X., 2014, Exceptional preservation of macrofossils from the Ediacaran Lantian and Miaohe biotas, South China: PALAIOS, v. 29, p. 129-136.

WESTRICH, J.T., AND BERNER, R.A., 1984, The role of sedimentary organic matter in bacterial sulfate reduction: The G model tested: Limnology and Oceanography, v. 29, p. 236-249.

WILBY, P.R., CARNEY, J.N., AND HOWE, M.P.A., 2011, A rich Ediacaran assemblage from eastern Avalonia: Evidence of early widespread diversity in the deep ocean: Geology, v. 39, p. 655-658.

WILKIN, R.T., AND BARNES, H.L., 1997, Formation processes of framboidal pyrite: Geochimica et Cosmochimica Acta, v. 61, p. 323-339, doi: 10.1016/S0016-7037(96)00320-1.

1287 WILLIAMS, H., AND KING, A.F., 1979, Trepassey Map Area, Newfoundland: Map Memoir of
1288 the Canada Geological Survey, 24 p.
1289 WILSON, L.A., AND BUTTERFIELD, N.J., 2014, Sediment effects on the preservation of Burgess
1290 Shale-type compression fossils: PALAIOS, v. 29, p. 145-154, doi:
1291 10.2110/palo.2013.075.
1292 WOOD, D.A., DALRYMPLE, R.W., NARBONNE, G.M., GEHLING, J.G., AND CLAPHAM, M.E.,
1293 2003, Paleoenvironmental analysis of the late Neoproterozoic Mistaken Point and
1294 Trepassey formations, southeastern Newfoundland: Canadian Journal of Earth
1295 Sciences, v. 40, p. 1375-1391.
1296 WOOD, R.A., POULTON, S.W., PRAVE, A.R., HOFFMANN, K.H., CLARKSON, M.O., GUILBAUD,
1297 R., LYNE, J.W., TOSTEVIN, R., BOWYER, F., PENNY, A.M., CURTIS, A., AND
1298 KASEMANN, S.A., 2015, Dynamic redox conditions control late Ediacaran metazoan
1299 ecosystems in the Nama Group, Namibia: Precambrian Research, v. 261, p. 252-271,
1300 doi: 10.1016/j.precamres.2015.02.004.
1301 XIAO, S., SCHIFFBAUER, J.D., MCFADDEN, K.A., AND HUNTER, J., 2010, Petrographic and
1302 SIMS pyrite sulfur isotope analyses of Ediacaran chert nodules: Implications for
1303 microbial processes in pyrite rim formation, silicification, and exceptional fossil
1304 preservation: Earth and Planetary Science Letters, v. 297, p. 481-495, doi:
1305 10.1016/j.epsl.2010.07.001.
1306 YUAN, X., CHEN, Z., XIAO, S., ZHOU, C., AND HUA, H., 2011, An early Ediacaran assemblage
1307 of macroscopic and morphologically differentiated eukaryotes: Nature, v. 470, p. 390-
1308 393.
1309 ZAKREVSKAYA, M., 2014, Paleoecological reconstruction of the Ediacaran benthic
1310 macroscopic communities of the White Sea (Russia): Palaeogeography,
1311 Palaeoclimatology, Palaeoecology, v. 410, p. 27-38.

ZHU, M., GEHLING, J.G., XIAO, S., ZHAO, Y.-L., AND DROSER, M.L., 2008, Eight-armed Ediacara fossil preserved in contrasting taphonomic windows from China and Australia: Geology, v. 36, p. 867-870.

FIGURES AND CAPTIONS

FIGURE 1—Locality map of late Ediacaran fossil sites in this study. **A**) Newfoundland, eastern Canada. **B**) The Avalon and Bonavista peninsulas, with the Catalina Dome and Mistaken Point. **C–D**) Geological map and stratigraphic column of the Catalina Dome. **E–F**) Geological map and stratigraphic column of the Mistaken Point region. Dates from Benus (1988) and Van Kranendonk et al. (2008). Stratigraphy after Williams and King (1979) and Hofmann et al. (2008).

FIGURE 2—Thin section images through selected fossil-bearing interfaces from the late Ediacaran of Newfoundland. See Supplementary Text for full locality and stratigraphic information regarding these surfaces. **A)** The MUN Surface, with a thin but continuous mineralized veneer beneath a normally graded tuff. **B)** Bed BR5, with a mineralized veneer almost 1mm thick within the lowermost portion of the over-bed. **C)** Bed H14, with a thin but continuous mineralized veneer. **D)** The E Surface, with a coarse-grained, chloritized tuff, and no mineralized veneer. **E)** Bed MEL 7, with a thin but continuous mineral veneer. **F)** A 'wisp' of framboidal pyrite within an under-bed, ~0.5mm beneath the fossil-bearing surface at Spaniard's Bay (SB).

FIGURE 3—Preservation of Ediacaran macrofossils on the BR5 fossil surface, Briscal Formation, Mistaken Point Ecological Reserve, Newfoundland. In each instance, Roman

numerals refer to specific sedimentary levels: (I) siltstone of the under-bed; (II) lower thin pyrite veneer; (III) upper thicker pyrite veneer separated from (II) by a thin (~100 μm) layer of sediment. **A–B**) Views of the bedding plane showing *Fractofusus* specimens coated by two distinct layers of iron oxide present. **C–E**) SEM BSE image of the pyritic veneer at the interface between under-bed and over-bed. **C**) Correspondence between the rusted levels in A and B and the original pyrite. **D**) Pyrite framboids with blocky pyrite overgrowths in level (III). **E**) Pristine pyrite framboids with no blocky overgrowths in level (II).

FIGURE 4—Progressive oxidation of framboidal pyrite within thin sections through bedding surfaces yielding Ediacaran macrofossils from Newfoundland, as revealed by SEM BSE images. **A**) Unweathered pyrite framboids from a fresh section through the BR5 surface (veneer level II of Fig. 3). **B**) Pyrite framboids with blocky pyrite overgrowths from the BR5 surface (veneer level III of Fig. 3). **C**) Iron oxide spheroids (replacing pyrite framboids) within a thin section from a section of the BR5 surface that has been exposed for several years (compare with A and B). **D**) Close up of iron oxide replacement of framboids within the BR5 surface veneer. Original framboidal textures are still visible, but EDS confirms that no original pyrite remains (Supp. Fig. 7). **E**) Blocky pyrite framboids (white) being replaced by iron oxide (light grey) within a single thin section field of view, LC6 surface. **F**) Relict framboids with blocky pyrite overgrowths from the LC13 surface. **G**) Zoned iron oxide spheroids at the interface between substrate and tuff on the MUN Surface. **H**) Spheroidal structures at the interface between substrate and tuff on the H14 (= LC5) bedding plane, preserved as unidentified aluminium-rich silicates (Supp. Fig. 8). Details of surface stratigraphic positions and paleontological attributes can be found in the Supplementary Text.

FIGURE 5—Electron microprobe elemental maps of three Newfoundland fossil-bearing surfaces, showing (from left) the mapped region, and elemental weight percent values for silicon (Si), iron (Fe), and sulfur (S). Maps reveal the distribution of spherical minerals, which are either composed of pyrite (bed BR5), iron oxides (MUN), or both (LC6) amongst a siliciclastic matrix. Note that the BR5 map displays only the upper levels of the over-bed pyritic veneer and a discrete layered iron oxide crust that appears to have formed as a result of modern weathering over the exposed surface. In sample LC6, framboids at higher levels within the veneer have been oxidised (upper right of image), while those closer to the under-bed remain pyritic.

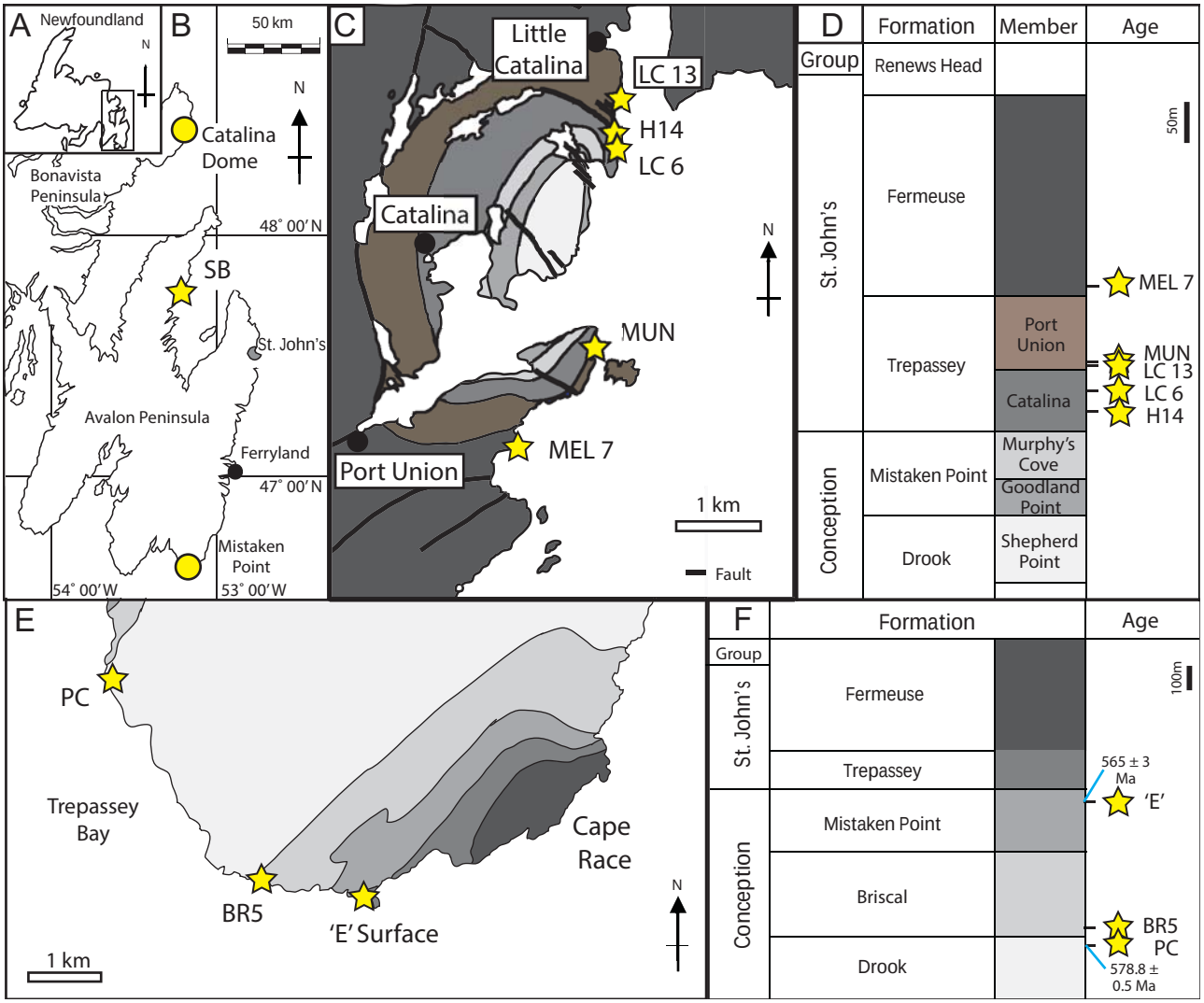
A
Newfoundland
N
B
50 km
N
Catalina
Dome
Bonavista
Peninsula
48° 00′ N
SB
St. John's
Avalon Peninsula
Ferryland
47° 00′ N
Mistaken
Point
54° 00′ W
53° 00′ W
C
Little
Catalina
LC 13
H14
LC 6
Catalina
N
MUN
MEL 7
Port Union
1 km
Fault
D
Formation
Member
Age
Group
Renews Head
Fermeuse
Trepassey
Port
Union
Catalina
Murphy's
Cove
Goodland
Point
Mistaken Point
Shepherd
Point
Drook
St. John's
Conception
50m
MEL 7
MUN
LC 13
LC 6
H14
E
PC
Trepassey
Bay
Cape
Race
BR5
'E' Surface
N
1 km
F
Formation
Age
Group
Fermeuse
Trepassey
Mistaken Point
Briscal
Drook
St. John's
Conception
100m
565 ± 3
Ma
'E'
BR5
PC
578.8 ±
0.5 Ma

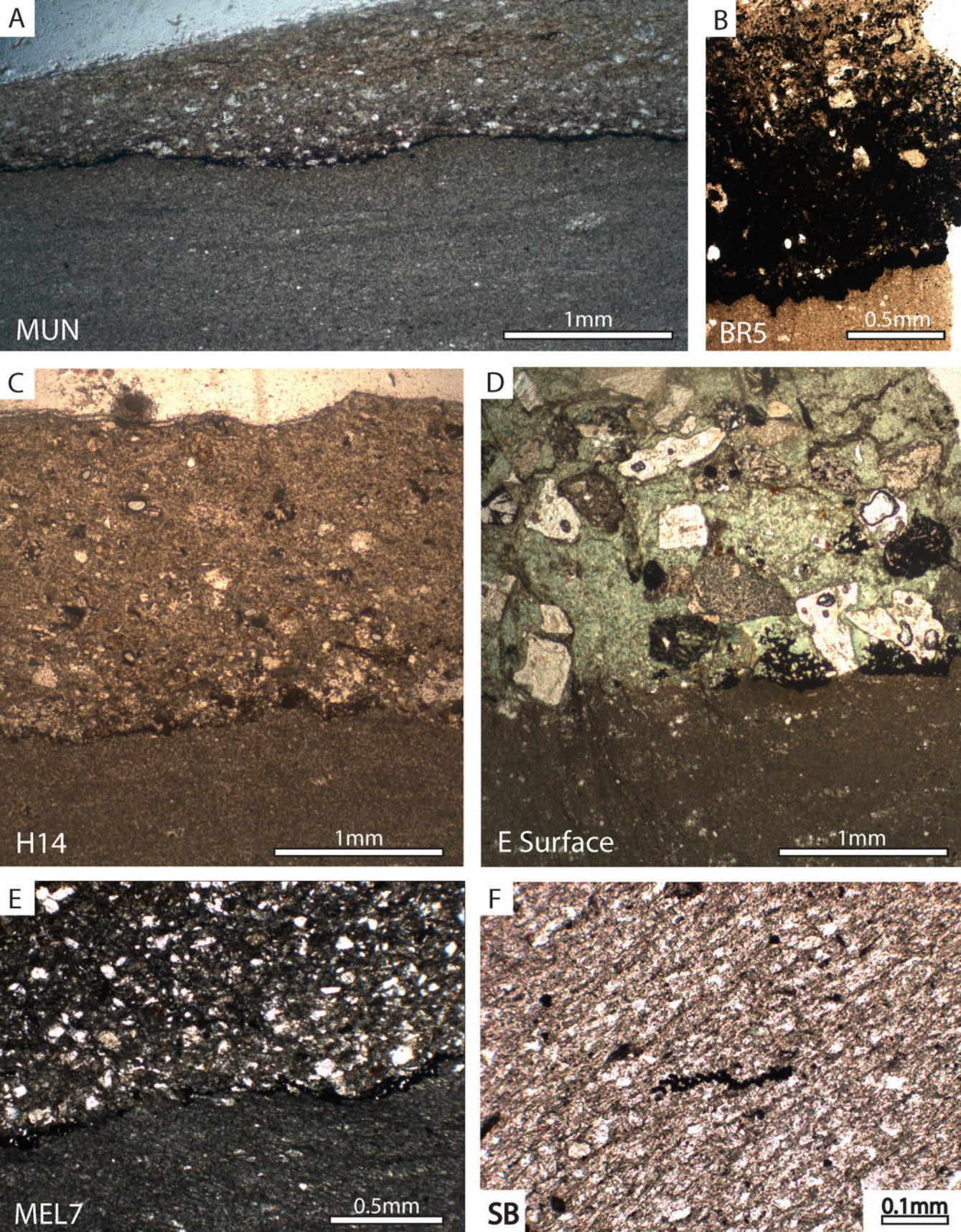
A
MUN
1mm
B
BR5
0.5mm
C
H14
1mm
D
E Surface
1mm
E
MEL7
0.5mm
F
SB
0.1mm

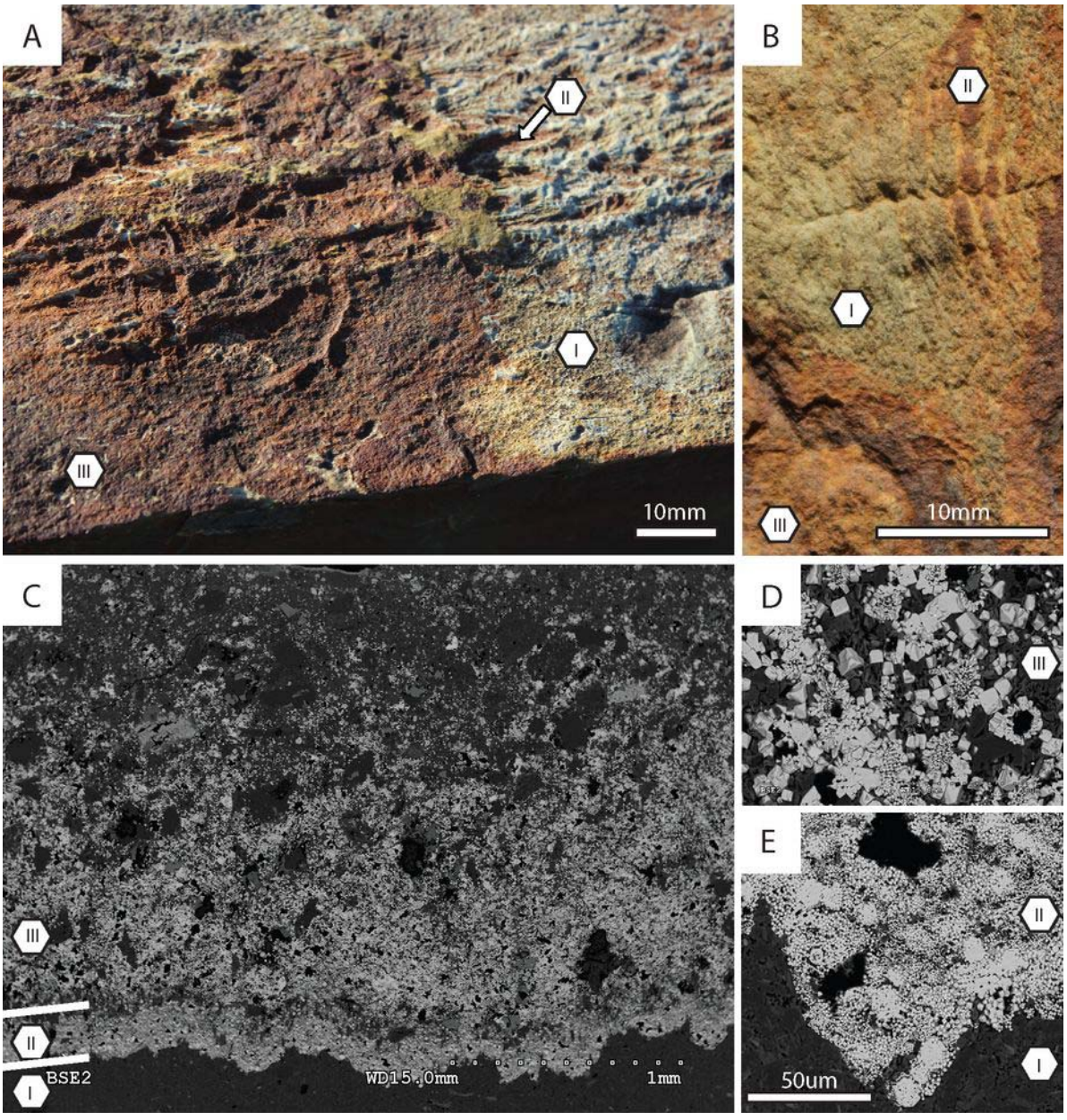
A
II
I
III
10mm
B
II
I
III
10mm
C
III
II
I
BSE2
WD15.0mm
1mm
D
III
E
II
I
50um

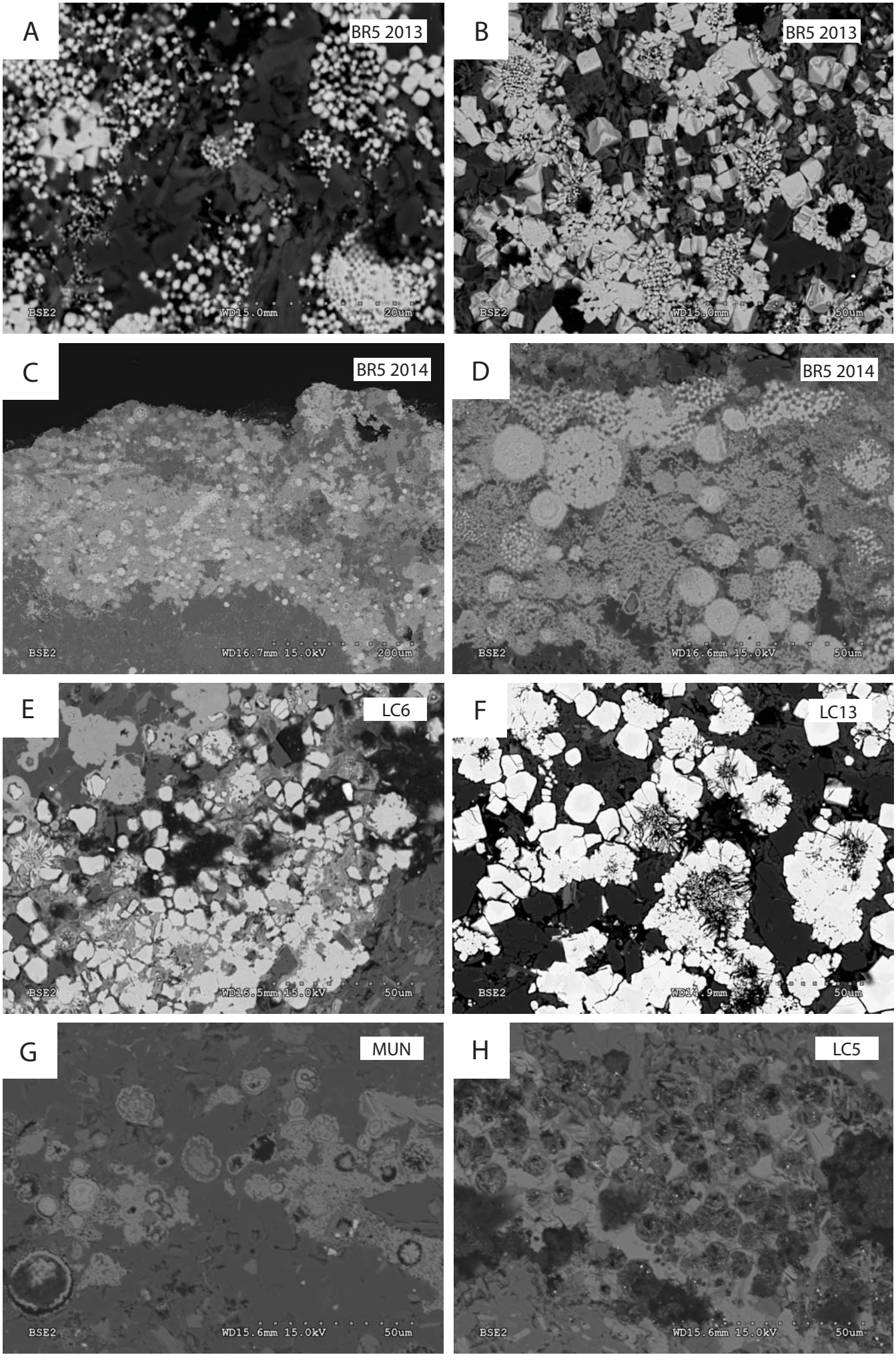
A
BR5 2013
BSE2
WD15.0mm
20um
B
BR5 2013
BSE2
WD15.0mm
50um
C
BR5 2014
BSE2
WD16.7mm 15.0kV
200um
D
BR5 2014
BSE2
WD16.6mm 15.0kV
50um
E
LC6
BSE2
WD16.5mm 15.0kV
50um
F
LC13
BSE2
WD14.9mm
50um
G
MUN
BSE2
WD15.6mm 15.0kV
50um
H
LC5
BSE2
WD15.6mm 15.0kV
50um

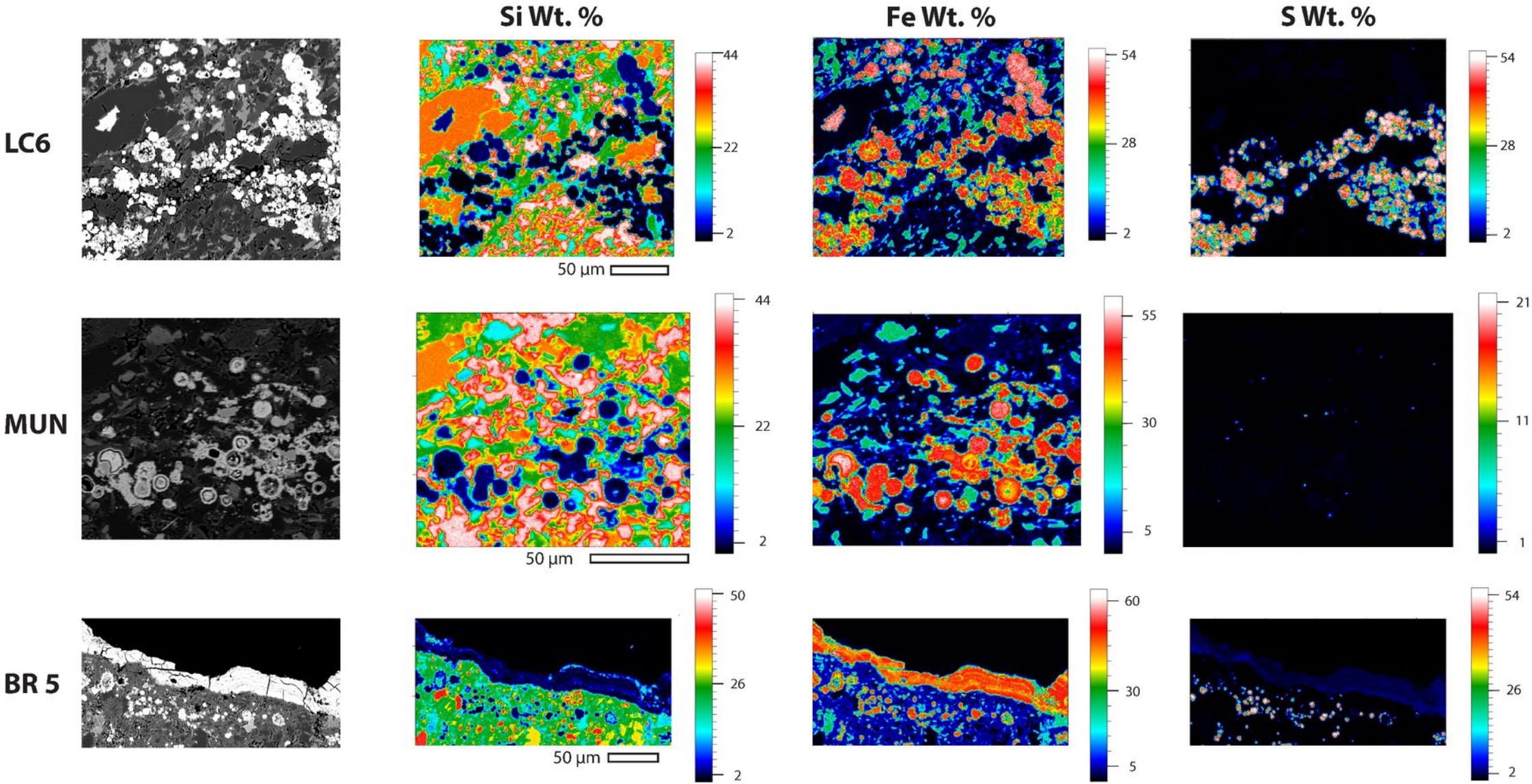
Si Wt. %
Fe Wt. %
S Wt. %
LC6
MUN
BR 5
44
22
2
54
28
2
54
28
2
50 µm
44
22
2
55
30
5
21
11
1
50 µm
50
26
2
60
30
5
54
26
2
50 µm